Contract No:

This document was prepared in conjunction with work accomplished under Contract No. DE-AC09-08SR22470 with the U.S. Department of Energy (DOE) Office of Environmental Management (EM).

Disclaimer:

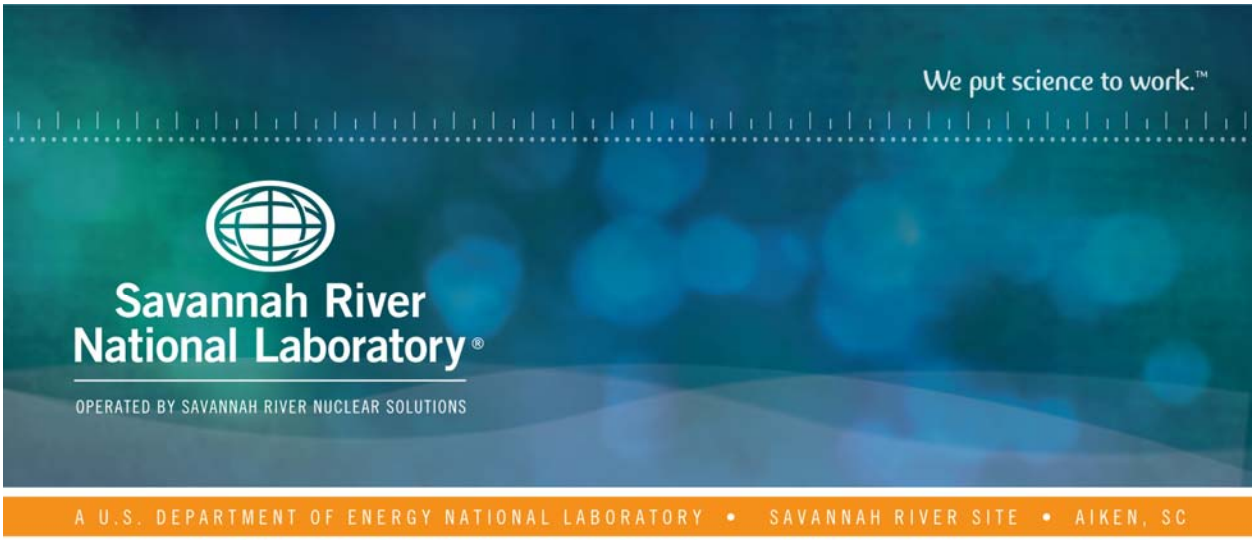

Investigation of Thermolytic Hydrogen Generation Rate in Tank 28 and Tank 39 Samples

C.J. Martino

J.M. Pareizs

W.H. Woodham

October 2019

SRNL-STI-2019-00411, Revision 0

DISCLAIMER

Printed in the United States of America

Prepared for
U.S. Department of Energy

SRNL-STI-2019-00411
Revision 0

Keywords: *Tank Farm, DWPF Recycle, Alternate Reductant*

Retention: *Permanent*

Investigation of Thermolytic Hydrogen Generation Rate in Tank 28 and Tank 39 Samples

C.J. Martino
J.M. Pareizs
W.H. Woodham

October 2019

Prepared for the U.S. Department of Energy under contract number DE-AC09-08SR22470.

Savannah River National Laboratory®
OPERATED BY SAVANNAH RIVER NUCLEAR SOLUTIONS

REVIEWS AND APPROVALS

AUTHORS:

_____
C.J. Martino, Process Technology Programs

_____
J.M. Pareizs, Process Technology Programs

_____
W.H. Woodham, Process Technology Programs

TECHNICAL REVIEW:

_____
C.L. Crawford, Advanced Characterization and Processing,
Design Verification by Document Review per E7 2.60

APPROVAL:

_____
F.M. Pennebaker, Customer Program Manager, Chemical Processing Technologies

_____
S.D. Fink, Director, Chemical Processing Technologies

_____
J.E. Occhipinti, Manager, Tank Farm Facility Engineering

ACKNOWLEDGEMENTS

The authors appreciate and sincerely thank the other scientists, engineers, and technicians that contributed to this work. Equipment setup and operation in the Shielded Cells, as well as analytical sample preparation, was accomplished by Nan Stanley, Michelle Edwards, Monica Jenkins, Rita Sullivan, Taylor Rush, Dee Wheeler, Julie Fawbush, and Kevin Haupfear. Thanks to them and the other Shielded Cells technicians, managers, and other support staff for the safe operation of these tests. Additional thanks go out to Tommy Edwards for statistical support and David Newell for equipment setup support. Various scientists and technicians in the Analytical Development section supported this work, including Amy Ekechukwu, Tom White, Nathan Wyeth, and Mark Jones. The primary customer engineers involved with shaping this testing were Christie Sudduth, Grace Chen, Tom Colleran, and Bill Holtzscheiter.

EXECUTIVE SUMMARY

This report contains hydrogen generation rate (HGR) measurements of Tank 28 and Tank 39 radioactive samples with and without added glycolate as a function of temperature. The objective of the Tank 28 and Tank 39 HGR measurements is to extend the knowledge from previous sample thermolysis HGR measurements and augment simulant testing for developing models for the Savannah River Site (SRS) Concentration, Storage, and Transfer Facilities (CSTF) thermolysis HGR with and without added glycolate. Tank 28 testing is applicable to concentrated salt supernate, legacy organic compounds resulting from the F-Canyon processes and boiling in the 3H-Evaporator System. Tank 39 testing is applicable to moderately concentrated salt supernate and organic compounds in fresh waste from the H-Canyon processes. For HGR tests with added sodium glycolate, the glycolate concentrations added to Tank 28 (500 mg/L) and Tank 39 (2000 mg/L) are based on concentrations expected to result in quantifiable HGR between temperatures of 70 °C and the atmospheric pressure boiling point. The added glycolate is much higher than the expected future glycolate concentrations in Tank 28, Tank 39, and similar CSTF tanks.

The following are key results from the Tank 28 HGR testing.

- For the sample without added glycolate, the first several HGR measurements at 70, 85, and 100 °C showed little increase over the temperature range, measuring approximately 6.7×10^{-7}, 6.1×10^{-7}, and 8.1×10^{-7} $ft^3\ h^{-1}\ gal^{-1}$ (cubic feet of hydrogen gas per hour per gallon of tank waste supernate), respectively. Upon increasing the temperature to the Tank 28 sample boiling point, 124.8 °C, the thermolytic HGR increased to 6.27×10^{-6} $ft^3\ h^{-1}\ gal^{-1}$. A second 70 °C HGR measurement was then performed, which showed a notable decline to 1.3×10^{-7} $ft^3\ h^{-1}\ gal^{-1}$.
- Using the measurements at 100 °C, boiling at 124.8 °C, and the second measurement at 70 °C, the activation energy without added glycolate is 80 kJ/mol.
- The HGR with 500 mg/L of added glycolate at 70, 85, 100, and 124.8 °C were 1.42×10^{-6}, 3.02×10^{-6}, 1.17×10^{-5}, and 1.42×10^{-4} $ft^3\ h^{-1}\ gal^{-1}$, respectively.
- Using the measurements at 85 °C and above, the activation energy with 500 mg/L of added glycolate is 115 kJ/mol. Factoring out the thermolytic HGR from the sample material and considering only the thermolytic HGR from 500 mg/L of glycolate in the solution (at 70 °C and above) the activation energy is 108 kJ/mol.
- For the test without added glycolate, methane was generated at levels near or below the 14 ppmv (5.7×10^{-7} $ft^3\ h^{-1}\ gal^{-1}$) Limit of Quantification (LOQ) during boiling. Methane was not detected for the test with 500 mg/L added glycolate. Carbon dioxide and nitrous oxide were also released during the testing without and with added glycolate.

The following are key results from the Tank 39 HGR testing.

- For the sample without added glycolate, the 70, 85, and 100 °C HGR measurements (7×10^{-8}, 7×10^{-8}, and 8×10^{-8} $ft^3\ h^{-1}\ gal^{-1}$, respectively) all showed decreasing trends. The HGR measurement at the boiling condition of 105.3 °C was 1.4×10^{-7} $ft^3\ h^{-1}\ gal^{-1}$. The activation energy was not calculated since quasi-steady state HGR values were not indicated in most experiments.
- The HGR with 2000 mg/L of added glycolate at 70, 85, 100, and 105.5 °C were 8×10^{-8}, 1.9×10^{-7}, 8.4×10^{-7}, and 3.74×10^{-6} $ft^3\ h^{-1}\ gal^{-1}$, respectively.
- Using the measurements at 85 °C and above, the activation energy with 2000 mg/L of added glycolate is 153 kJ/mol. Factoring out the thermolytic HGR from the sample material and considering only the thermolytic HGR from 2000 mg/L of glycolate in the solution, the activation energy is 178 kJ/mol.

- No methane or nitrous oxide was detected during the Tank 39 sample testing without and with added glycolate. Carbon dioxide was observed during testing.

TABLE OF CONTENTS

LIST OF TABLES

LIST OF FIGURES

LIST OF ABBREVIATIONS

CI	Confidence Interval
CPC	Chemical Processing Cell
CSTF	Concentration, Storage, and Transfer Facilities
DAC	Data Acquisition and Control
DMA	Direct Mercury Analysis
DSA	Documented Safety Analysis
DWPF	Defense Waste Processing Facility
E_a	Activation Energy
EPA	Environmental Protection Agency
GC	Gas Chromatograph
HGR	Hydrogen Generation Rate
HMDSO	Hexamethyldisiloxane
ICA	Ion Chromatography for Anions
ICP-AES	Inductively Coupled Plasma – Atomic Emissions Spectroscopy
ICP-MS	Inductively Coupled Plasma – Mass Spectroscopy
LOD	Limit of Detection
LOQ	Limit of Quantification
LTAD	Low Temperature Aluminum Dissolution
MMHg	Methylmercury
MS&E	Measurement Systems and Equipment
M&TE	Measuring and Test Equipment
n.d.	Not determined
NGA	Nitric-Glycolic Acid
PISA	Potential Inadequacy in the Safety Analysis
RSD	Relative Standard Deviation
SPF	Saltstone Processing Facility
SRNL	Savannah River National Laboratory
SRR	Savannah River Remediation
SRS	Savannah River Site
SVOA	Semivolatile Organics Analysis
TC	Total Carbon
TIC	Total Inorganic Carbon
TOC	Total Organic Carbon
TMS	Trimehtylsilanol
TTQAP	Task Technical and Quality Assurance Plan
TTR	Technical Task Request
VOA	Volatile Organics Analysis
WTP	Waste Treatment Plant

1.0 Introduction

1.1 The Issue of Thermolytic Hydrogen Generation

In February 2017, Savannah River Remediation (SRR) declared a Potential Inadequacy in the Safety Analysis (PISA) in each of three Savannah River Site (SRS) Liquid Waste facilities: Concentration, Storage, and Transfer Facilities (CSTF),[1] Saltstone Processing Facility (SPF),[2] and the Defense Waste Processing Facility (DWPF).[3] The PISAs relate to how organics can impact the radiolytic and thermolytic production of hydrogen, which is a flammable gas.

With the implementation of the Nitric-Glycolic Acid (NGA) flowsheet at DWPF, small amounts of glycolate will transfer into the SRS CSTF from the DWPF recycle stream. A literature survey indicated that glycolate can produce hydrogen via thermolytic reactions.[4] Work performed for the Hanford Reservation tank waste programs indicated that glycolate decomposition in high pH solutions containing soluble aluminum generates hydrogen.[5-6] A prior analysis of this literature data predicted the expected influence of glycolate on radiolytic and thermolytic hydrogen generation in the SRS CSTF, SPF, and DWPF.[7]

1.2 Documents Related to This Task

To address these needs, SRR issued a Technical Task Request (TTR) requesting that Savannah River National Laboratory (SRNL) perform simulant and actual waste testing to support thermolytic Hydrogen Generation Rate (HGR) determination for CSTF processes.[8] This report covers a portion of the data gathered as Task 2 of the TTR, specifically addressing data from radioactive waste spiked with glycolate. A Task Technical and Quality Assurance Plan (TTQAP) further defines the radioactive-waste and simulated-waste testing.[9] Finally, two Run Plans give test details specific to the HGR testing of radioactive waste samples from Tank 28 and Tank 39.[10-11] Testing was performed in flow systems as deemed most appropriate for use with these samples.

1.3 Previous Thermolytic HGR Measurements at SRNL

SRNL conducted initial research to determine the thermolytic HGR with simulated and radioactive waste. Gas chromatography methods were developed and used with air-purged flow systems to quantify hydrogen generation from heated simulated and radioactive waste at rates applicable to the CSTF Documented Safety Analysis (DSA). Initial testing included a measurement of HGR on waste from Tank 38 and simulated waste with the most common SRS CSTF organics at temperatures up to 140 °C.[12] HGR measurements of Tank 50 samples with and without additives (not including glycolate) were performed using a sealed measurement system.[13] After redesign of a flow system to minimize impacts from glass and stainless steel components to the extent possible, HGR was quantified for a Tank 38 sample with and without 1570 mg/L glycolate and for a Tank 50 sample with 350 mg/L glycolate.[14] Measurement with Tank 22 samples with and without 120 mg/L of added glycolate showed none to minimal thermolytic HGR in that dilute sample matrix with the higher detection limits of the flow system.[15] In addition, considerable testing with non-radioactive simulants was performed to screen tank farm organics for thermolytic production of hydrogen, quantify thermolytic HGR from glycolate and the most reactive tank farm organics over the range of CSTF conditions, and develop reaction models for thermolytic HGR applicable to SRS waste.[16-19]

1.4 Test Objectives

This report contains HGR measurements of Tank 28 and Tank 39 radioactive samples with and without added glycolate. The primary goals for Tank 28 and Tank 39 HGR measurements are as follows:

- to extend the knowledge from the previous sample measurements[12-15] to tanks that have different levels of salts and different sources of organic compounds,
- to augment simulant testing for thermolytic HGR of CSTF organics, and
- to provide data to confirm the reaction models for thermolytic HGR of glycolate in the CSTF.

The purpose of the heated measurements of Tank 28 and Tank 39 samples without added glycolate is to investigate the thermolytic HGR of the mixture of organic compounds currently residing in the tank supernates. SRR issued a report that outlined the justification for the tanks selected.[20] In an effort to represent thermolytic HGR across the CSTF, Tank 28 and Tank 39 were selected because they differed in several important ways from waste samples that were already investigated.

Tank 28 was chosen for testing because it met a variety of criteria not met by some of the previous samples used for thermolysis HGR testing. Tank 28 is a highly concentrated supernate that should allow for testing at higher temperatures than were attained in previous experiments due to its elevated atmospheric pressure boiling point. Previous samples of Tank 28 saltcake free liquid had a relatively high organic carbon concentration that was not attributable to formate or oxalate.[21] This other organic carbon may potentially contribute to thermolytic HGR. Tank 28 contains material that was processed in the 1F and 2F-Evaporator Systems, resulting from F-Canyon processes, which has yet to be directly studied in previous thermolytic HGR tests. The high salt concentration also seeks to represent HGR in the 3H-Evaporator System tanks, which do not have as high an organic carbon concentration as Tank 28.

Tank 39 was chosen for testing because of the blend of organics it may contain as a result of receiving transfers directly from the H-Canyon Facility. Solids in the tank were expected to not impact thermolytic HGR. The thermolytic production of hydrogen is assumed to be primarily a supernate phenomenon, thereby suggesting that HGR measurements with present sludge solids are not necessary to capture thermolytic HGR contributions.[22]

A relationship of the impact of glycolate on thermolytic hydrogen generation in the SRS waste tanks is being developed through simulant testing. One objective for measurement of thermolytic HGR of Tank 28 and 39 samples with added glycolate is to provide additional confirmation of the simulant testing.

1.5 Thermolytic Hydrogen Generation Background

A background of thermolytic hydrogen generation applicable to current CSTF organic compounds and future additions of glycolate are detailed elsewhere.[7, 12] In work designed to support flammability calculations at the Hanford Waste Treatment Plant (WTP), Hu developed an empirical model describing the thermolytic production of hydrogen from organic molecules as a function of temperature, organic carbon content, and aluminum content.[22] In 2017, Crawford and King used observations and glycolate destruction rate data generated by Ashby et al.[5] to develop a rate expression for hydrogen generation due to glycolate thermolysis.[7] The glycolate thermolysis HGR model was predicted to be a function of temperature, glycolate, nitrite, and aluminum concentration and to have an unconfirmed inverse proportionality to hydroxide concentration.

Simulant work performed at SRNL on thermolysis of glycolate and CSTF organic compounds at conditions applicable to SRS waste has determined relationships that differ from the rate expressions generated by Hu and by Crawford and King.[19] Most strikingly, most of the SRNL testing for glycolate and CSTF organic compounds showed a direct relationship to hydroxide concentration. While hydroxide is a major component of both SRS and Hanford tank waste, hydroxide did not appear in Hu's rate expression and had the opposite functionality relative to expectations in Crawford and King's rate expression. The SRNL simulant testing maintained the direct relationship between concentration of the organic compound of interest and the thermolytic HGR.

1.6 Glycolate Concentration Applicable to HGR Testing

For the previous thermolytic HGR testing with Tank 22, which is the receipt tank for DWPF recycle, the typical glycolate concentration applicable to Tank 22 was estimated as 120 mg/L based on considerations

of historic DWPF recycle system samples and NGA flowsheet testing.[23] Similarly, the glycolate concentration applicable to the Tank 38 testing was estimated as 1570 mg/L based on historic observations of formate in the 2H-Evaporator System.[14] Likewise, the glycolate concentration applicable to the Tank 50 testing was determined to be 350 mg/L based on the highest formate concentration measured in Tank 50 samples from recent salt processing.[14]

Similar or analogous approaches, however, cannot be used to determine the applicable glycolate concentrations for use in Tank 28 and Tank 39 thermolysis HGR testing. Tank 28 will be a salt recovery tank. For the worst case of using DWPF recycle as the saltcake dissolution fluid, the resulting mixture will have significantly less than the 120 mg/L glycolate used in the Tank 22 testing. In the use of the Tank 28 sample to represent the concentrated 3H-Evaporator System material, the DWPF recycle material will not routinely be sent to the 3H-Evaporator System, leading to very low or no glycolate concentrations in those tanks. Similarly, Tank 39 is used as a receipt tank of new waste from the H-Canyon Facility and is not expected to have any appreciable glycolate concentration in the future. If Tank 28 and Tank 39 glycolate concentrations were to be based on expected future concentrations, the impacts of the very small added glycolate are expected to be too low to provide useful data for glycolate model comparisons. Thus, the concentration of glycolate added in the Tank 28 and Tank 39 tests are based upon what would provide the most useful measured values rather than matching future expected glycolate levels in those tanks or tanks containing similar waste.

Prior to testing, it was predicted that Tank 28 without added glycolate may have a significant HGR due to its previously measured organic carbon content and its relatively high concentration of hydroxide and total salt. It was important that the amount of glycolate added be adequate to differentiate the HGR due to glycolate thermolysis from the HGR due to thermolysis of other Tank 28 organics. Glycolate should be added at a concentration targeting the contribution to HGR from glycolate thermolysis of at least three-times the HGR of Tank 28 without added glycolate. If possible, glycolate should also be added at a concentration above the analytical detection limit of Ion Chromatography for Anions (ICA) in the Tank 28 matrix, which was expected to be approximately 200 mg/L. To meet the test objectives, it was also important that glycolate be added to the Tank 28 sample at a concentration that would allow for the study of the impact of glycolate on HGR while not being so high as to challenge flammability controls on the test system. For this case, 500 mg/L of added glycolate was calculated and proposed as a target glycolate concentration to allow for the measurement of HGR from 70 °C (prediction of 2×10^{-6} ft^3 h^{-1} gal^{-1}) to the predicted atmospheric-pressure boiling temperature of 122 °C (prediction of 3×10^{-4} ft^3 h^{-1} gal^{-1}).[19]

Compared to other tank supernates, Tank 39 was expected to have moderate concentrations of hydroxide and other salts. To meet the test objectives, it was important that glycolate be added to the Tank 39 sample at a concentration that would allow for the study of the impact of glycolate on HGR. For this case, 2000 mg/L of added glycolate was expected to allow for the measurement of HGR from 70 °C (prediction of 1.6×10^{-7} ft^3 h^{-1} gal^{-1}) to an assumed atmospheric-pressure boiling temperature (prediction of 5 to 6×10^{-6} ft^3 h^{-1} gal^{-1}).[19]

2.0 Experimental

2.1 Shielded Cells Flow System Apparatus

2.1.1 Description of Apparatus

The flow-system apparatus used in the Tank 28 and Tank 39 thermolytic HGR testing in the Shielded Cells is identical to the system used for Tank 22, Tank 38, and Tank 50 thermolytic HGR testing with the exception that the glass funnel for sample addition was removed.[14-15] The apparatus was based on the simulant testing flow system being used for Task 1 of the TTR and TTQAP.[8-9] The apparatus combined design elements from equipment used for previous one liter and four liter sludge batch qualification

Chemical Processing Cell (CPC) testing.[24-25] The vessel holding the radioactive waste sample and the sealing lid assuring capture of gases during testing was made of Teflon®, with an internal volume of approximately 1.2 liters. Use of a flow-through system with minimal headspace is consistent with the HGR measurement apparatus recommended and developed for qualification of radioactive-waste feeds at the Hanford WTP, although dimensions are larger for this application.[26-27] Teflon® fluoropolymer was used for HGR flow-system measurements to minimize potential interferences from performing tests in glass or stainless-steel vessels and was chosen based on literature preparations and recommendations from simulant testing.[5, 17]

Figure 2-1 contains two photographs of the HGR measurement system. The photograph on the left is the system with the stainless-steel pot prior to its use in the Low Temperature Aluminum Dissolution (LTAD tests).[28] The photograph on the right is the same system but with a Teflon® pot installed in SRNL Shielded Cells, A Block Cell 2 (note that the insulation is not shown in the photograph). A separate Teflon® pot is installed for each tank sample to be tested.

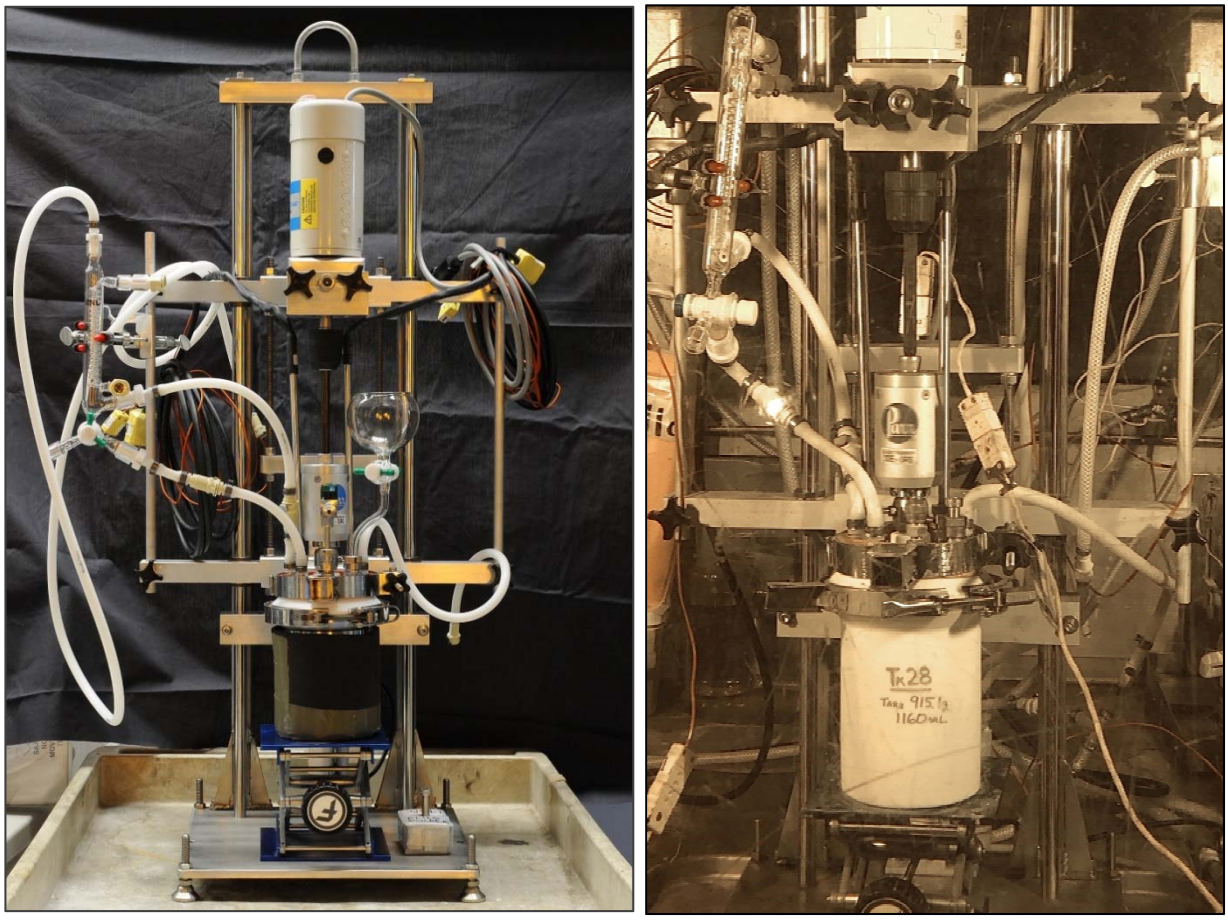

Figure 2-1. HGR measurement flow system prepared for installation (left) and in operation (right).

Heating was provided using two 0.375-inch diameter Alloy 800 heating rods powered by an automated direct current power supply (TDK-Lambda Genesys, GEN150-10). Mixing was controlled using a mixer system consisting of a Servodyne mixing head coupled to an agitator shaft via a Parr high torque magnetic drive. A Teflon® pitched turbine impeller was attached to a Teflon® agitator shaft. The slurry was

continually stirred over the course of the testing. Purge gas was controlled using an MKS Model 647 Multi Gas Controller and MKS Model 1179 Flow Controller. An offgas condenser allowed condensate to reflux into the reactor containing the sample material. Non-condensable gas exiting the condenser was sampled by a dedicated Agilent 3000A dual column micro gas chromatograph (GC), as described in further detail in a later subsection. A data acquisition and control (DAC) system was utilized for control of the heating rods, mixing, and purge gas flow and for automated data logging. A schematic depicting integration of the primary components of the HGR measurement flow system apparatus is given in Figure 2-2.

Additional details about the flow-system apparatus and its use is contained in the Tank 22 thermolytic HGR testing report.[15]

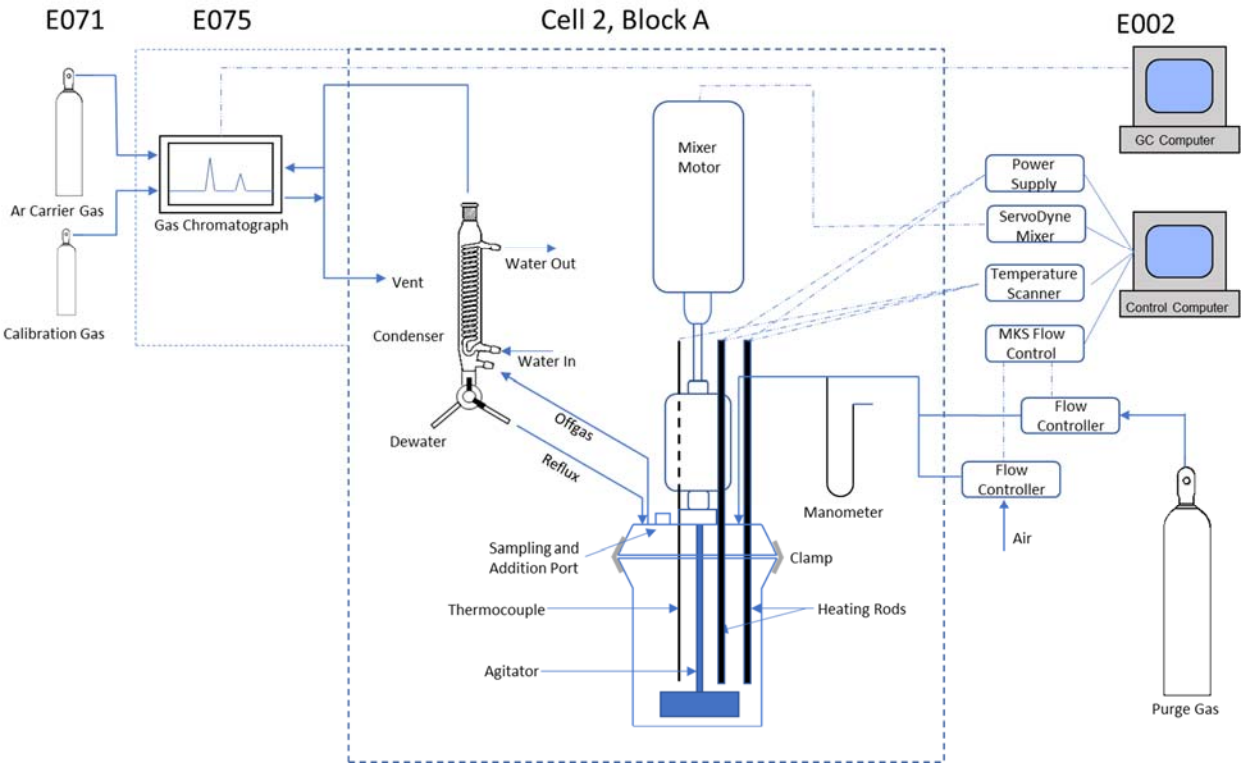

Figure 2-2. HGR measurement flow system used in Tank 28 and Tank 39 testing.

2.2 Test Protocol

2.2.1 Samples and Chemicals

A description of the Tank 28 and Tank 39 samples used in testing, along with the results of sample characterization, is contained in Section 3.0. Two separate 1.06 L aliquots for each of the two tank samples were used during testing, for a total of four sample aliquots. The use of separate sample aliquots for the tests without and with added sodium glycolate is similar to the method used for Tank 22 sample HGR testing and is in contrast with the method used for Tank 38 sample testing.[14-15]

Any salt crystals that could not be removed from the Tank 28 sampler or sample transfer tubing were not included as part of the as-received material and thus were not included in the HGR test. Salt crystals that were transferred into the Tank 28 sample bottle were split uniformly into the sample aliquots used in the

HGR testing and the sample analysis. Likewise, insoluble solids contained in the Tank 39 sample were split uniformly into the sample aliquots used in the HGR testing and the sample analysis.

The samples did not contain glycolate, so sodium glycolate (Alfa Aesar, 99.1 wt %) was added to the sample material to achieve the desired concentration, where applicable.

2.2.2 Flow System Testing Parameters

The parameters for flow-system testing of Tank 28 were as follows.

- Measurement apparatus: nominally 1 L flow system, fluoropolymer vessel with fluoropolymer lid. Total volume (liquid and gas) of approximately 1.2 L.
- Test sample: 3 L Tank 28 sample FTF-28-19-8
- Sample density: 1.462 g/mL at 26 °C
- Sample volume: approximately 1.06 L
- Sample mass: approximately 1550 g
- Glycolate addition, where applicable: 500 mg/L of glycolate (as sodium glycolate)
- Equipment total gas volume: approximately 140 mL
- Target measurement purge rate: 3 mL/min at standard conditions (1 atm and 21.1 °C). Higher rates of air without Kr tracer (10 to 80 mL/min) were used during periods of temperature adjustment. A lower rate of purge gas with Kr tracer (3 mL/min to 10 mL/min) was applied once the measurement temperature was attained.
- Expected minimum time to equilibrate for HGR measurement: It required approximately 3 hours to achieve three vapor space volume turn-overs at standard conditions and 3 mL/min purge rate.
- Condenser cooling water set point: 10 °C
- Condenser gas output temperature target: 10 to 30 °C (influenced by ambient shielded cell temperature)
- Heating rod temperature target: less than 20 °C above solution temperature when equilibrating at measurement temperature; less than 30 °C above solution temperature when heating to measurement temperature
- Mixer rate: nominally 100 to 300 rpm, or as needed for liquid mixing and foam control. Note that there was no visual confirmation of mixing or foaming.

The testing parameters for flow-system testing of Tank 39 were as follows.

- Measurement apparatus: nominally 1 L flow system, fluoropolymer vessel with fluoropolymer lid. Total volume (liquid and gas) of approximately 1.2 L.
- Test sample: Tank 39 sample HTF-39-19-1
- Sample density: 1.235 g/mL at 26 °C
- Sample volume: approximately 1.06 L
- Sample mass: approximately 1310 g
- Glycolate addition, where applicable: 2000 mg/L of glycolate (as sodium glycolate)
- Equipment total gas volume: approximately 140 mL
- Target measurement purge rate: 3 mL/min at standard conditions (1 atm and 21.1 °C). Higher rates of air without Kr tracer (e.g., 10 to 40 mL/min) were used during periods of temperature adjustment. A lower rate of purge gas with Kr tracer (3 mL/min) was applied once the measurement temperature was attained and the Kr measurement provided an indication that the test had proceeded for at least three vapor space volume turn-overs.
- Expected minimum time to equilibrate for HGR measurement: It required approximately 3 hours to achieve three vapor space volume turn-overs at standard conditions and 3 mL/min purge rate.
- Condenser cooling water set point: 10 °C

- Condenser gas output temperature target: 10 to 30 °C (influenced by ambient shielded cell temperature)
- Heating rod temperature target: less than 20 °C above solution temperature when equilibrating at measurement temperature; less than 30 °C above solution temperature when heating to measurement temperature
- Mixer rate: nominally 100 to 300 rpm, or as needed for liquid mixing and foam control. Note that there was no visual confirmation of mixing or foaming.

2.2.3 Flow System Testing Process

HGR measurements at a series of temperatures were performed on two aliquots of the Tank 28 sample, one without and one with the addition of sodium glycolate. Similarly, HGR measurements at a series of temperatures were performed on two aliquots of the Tank 39 sample, one without and one with the addition of sodium glycolate. The measurements were performed by holding the tank sample aliquots in a fluoropolymer vessel that allows for mixing, heating, temperature measurement, and gas measurement. Hydrogen, methane, carbon dioxide, nitrous oxide, and krypton (tracer) in the offgas were measured by a GC system. The offgas was carried to the GC by purge gas, which is a mixture containing 20 vol % oxygen, 0.5 vol % krypton tracer, and a balance of nitrogen. In parallel with HGR testing, portions of the original Tank 28 and Tank 39 samples without added glycolate were prepared and submitted for chemical analysis.

The HGR measurements of Tank 28 and Tank 39 sample material without glycolate were performed at a series of increasing temperatures from 70 °C to the atmospheric pressure boiling point of the material, followed by a measurement near ambient temperature. For the Tank 28 sample measurements without added glycolate, an additional 70 °C HGR measurement was added between the boiling and ambient temperature conditions. Because the HGR measurements are performed at a series of temperature hold points for a single sample aliquot, a risk exists that the measurements at the prior hold points can consume a portion of the reactant, potentially contributing to a low bias in the measurements at the subsequent hold points. The material was removed from the HGR measurement apparatus and sampled for post-HGR analysis. A separate aliquot of the sample and the desired concentration of glycolate (500 mg/L glycolate for Tank 28 and 2000 mg/L glycolate for Tank 39, added as sodium glycolate) was loaded into the apparatus, heated to 70 °C, measured for HGR, and sampled for initial glycolate content. Subsequent HGR measurements were performed at a series of increasing temperatures up to the atmospheric pressure boiling point of the material, followed by a measurement near ambient temperature. The material was removed from the HGR measurement apparatus and sampled for post-HGR analysis.

Testing was performed in the following order over a two-week period from June 3 to June 15, 2019:

Test 1: Tank 28 sample without added glycolate
Test 2: Tank 39 sample without added glycolate
Test 3: Tank 39 sample with 2000 mg/L of added glycolate
Test 4: Tank 28 sample with 500 mg/L of added glycolate

Step-by-step details of the testing process are included in Appendix A.

2.3 Data Collection

2.3.1 Gas Handling and Analysis (flow system)

Offgas from the tests was characterized using an Agilent series 3000 micro GC. Column-A collected data related to He, H_2, O_2, N_2, Kr, and CH_4, while column-B collected data related to CO_2 and N_2O. Due to limited GC sensitivity when using argon carrier gas (needed for hydrogen quantification), it was not possible to identify other oxides of nitrogen and carbon. The GC method was modified to quantify low

quantities of hydrogen. The instruments have previously been used to quantify offgas from DWPF CPC demonstrations which generally have significantly higher gas generation rates. To quantify the low concentrations of hydrogen, sample injection times were increased by a factor of three relative to DWPF simulations. To improve sensitivity, the GC sensitivity mode was changed from normal to high. Because of these changes, the ability to accurately quantify oxygen and nitrogen has been significantly reduced relative to the semi-quantitative results generally seen in CPC simulations. Raw chromatographic data were acquired by the GC from the offgas stream samples using a separate computer interfaced to the data acquisition computer. Sampling frequency was approximately one chromatogram every eight minutes.

The GC was calibrated with a gas mixture containing 50 ppmv hydrogen, 100 ppmv methane, 20.0 vol % oxygen, 0.5 vol % krypton, 1.0 vol % carbon dioxide, 0.5 vol % nitrous oxide, and the balance nitrogen. It was assumed that the GC response (peak area) was linear and proportional to the gas concentration. This assumption was demonstrated to be appropriate for hydrogen with several other hydrogen-bearing gas standards.[12] The calibrations were verified prior to and after completing the week of flow-system testing. Five sets of calibration data were collected over the course of the Tank 28 and Tank 39 sample HGR tests. From each set of calibration measurements, the last 10 observations were considered for use in calibration. Details on use of the calibration data are contained in Appendix E.

The primary purge gas contained 0.5 vol% krypton, 20.0 vol% oxygen, and 79.5 vol% nitrogen. Air purge was also available and used to partially flush the system between measurement conditions. The Kr-bearing purge gas (as compared to air) served several purposes. First, by using the measured krypton concentration, one could determine if the headspace of the reaction vessel had been purged of air. Second, unlike air, the purge had no helium and hydrogen, which could interfere with quantification of hydrogen produced from radiolysis or thermolysis. Third, Kr measurements were used to adjust for bulk gas generation from the sample, air leakage into the system, and back-mixing at the GC.

The relationship identified in Equation 1 was used to calculate the HGRs. With this equation, it was assumed that flow out of the vessel was equal to flow into the vessel. The validity of this assumption was confirmed by checking that the measured Kr concentration was the same as the Kr concentration in the purge gas fed to the reaction vessel.

$$\boldsymbol{HGR = H2_{area} \times \frac{H2_{stdconc}}{H2_{stdarea}} \times \frac{Kr_{stdarea}}{Kr_{stdconc}} \times \frac{Kr_{purgegas}}{Kr_{area}} \times F_{in} \times \frac{\rho}{m} \times 8.126 \times 10^{-6}} \quad \text{Equation 1}$$

where,

HGR = H_2 generation rate, $ft^3 \cdot h^{-1} \cdot gal^{-1}$

$H2_{area}$ = GC H_2 response for a gas sample

$H2_{stdconc}$ = Concentration of H_2 calibration gas, ppmv

$H2_{stdarea}$ = Average of five GC responses from the H_2 calibration gas

F_{in} = flow of Kr-bearing purge gas into the reaction vessel, mL/min

ρ = density of sample, $g \cdot mL^{-1}$

m = mass of sample, g

8.126×10^{-6} = conversion factor and temperature adjustment, $ft^3 \cdot min \cdot mL \cdot cc^{-1} \cdot gal^{-1} \cdot ppmv^{-1} \cdot hr^{-1}$

$Kr_{purgegas}$ = Concentration of Kr in the purge gas, not including any supplemental air, vol %

Kr_{area} = GC Kr response for a gas sample

$Kr_{stdconc}$ = Concentration of Kr calibration gas, vol %

$Kr_{stdarea}$ = Average of five GC responses from the Kr calibration gas

The units of HGR are cubic feet of hydrogen gas per hour per gallon of tank waste supernate, or $ft^3\ h^{-1}\ gal^{-1}$. The gas volume basis of the HGR measurements reported in this document is at a standard condition of 25 °C and 1 atm to match the CSTF HGR calculation standard condition. Purge rates quoted in this document are at a standard condition of 21.1 °C and 1 atm to match the standard condition of the HGR measurement apparatus.

The software package GUM workbench[29] was used to determine the partial derivatives used to calculate the overall uncertainty for the above equations. The overall uncertainty (using these derivatives) and one sigma uncertainties in the variables was then used to calculate uncertainties for all the data points using the software package JMP Pro Version 11.2.1.[30]

Based on current and previous GC calibration data,[12] the Limit of Quantification (LOQ) for hydrogen was determined to be 2.3 ppmv. Using a simplified version of Equation 1,[a] the minimum LOQ corresponds to approximately $5.3\times10^{-8}\ ft^3\ h^{-1}\ gal^{-1}$ at the sample volume and purge rate used for Tanks 28 and 39 flow-system testing. The Limit of Detection (LOD) was determined to be 1.2 ppmv, which corresponds to approximately $2.8\times10^{-8}\ ft^3\ h^{-1}\ gal^{-1}$ for this testing. Measurements below the LOQ are semi-quantitative and should only be applied in a qualitative manner, such as representing general trends (i.e., increasing or decreasing with time). Measurements above the LOD but below the LOQ should be interpreted as positive indications of the presence of hydrogen as distinguishable from the GC baseline measurement. However, measurement uncertainty and bias are greatly increased when below the LOQ, and thus measurement values below the LOQ should not be used in calculations and comparisons.

SRNL evaluated the GC with 2 ppmv and 10 ppmv methane standards (balance air in both cases). The GC was unable to detect 2 ppmv methane. The 10 ppmv methane gas could be detected and quantified. Ten measurements of this calibration gas yielded a relative standard deviation of 15%. Based on the 10 ppm methane calibration gas, the GC's LOD is less than 10 ppmv. Using an Environmental Protection Agency (EPA)[31] and Taylor[32] based methodology, the methane LOQ is approximately 14 ppmv.

For Tank 28 and 39 HGR tests, a shift in the calibration data over time (as seen in Appendix E) required consideration. Both hydrogen and krypton calibration gas area measurements are seen to generally increase over the course of the two weeks of testing. Providing thermolytic HGR measurements for potential use in Safety Basis calculations is amongst the goals of this testing. For this reason, calibration anomalies that impact HGR measurements are included as a potential high bias in the measurements to maintain conservatism. Examining Equation 1, the calculation of HGR from GC measurements has the relationship of HGR as inversely proportional to the hydrogen calibration area and directly proportional to the krypton calibration area. Thus, to maintain conservatism, the lowest applicable hydrogen calibration areas and highest applicable krypton calibration areas were used. Overall, this approach resulted in an approximately 0% to 10% high bias in the reported HGR measurements.

2.3.2 Analytical Methods for Sample Analysis

The feeds and products of the HGR tests were analyzed by the following methods. Methods included Inductively Coupled Plasma – Atomic Emissions Spectroscopy (ICP-AES); Inductively Coupled Plasma – Mass Spectroscopy (ICP-MS); Direct Mercury Analysis (DMA), ICA; titration for total base, free hydroxide, and other base excluding carbonate; and Total Inorganic Carbon (TIC)/Total Organic Carbon (TOC), Volatile Organics Analysis (VOA) and Semivolatile Organics Analysis (SVOA). The ICA analysis for glycolate and other organic acid anions used an OnGuard™ II column to remove transition metals to improve the peak shape and ultimately the quantification of these anions.

[a] In Equation 1, the first three terms involving hydrogen simplify to the hydrogen measurement concentration in ppm. The four terms involving krypton simplify to unity.

2.4 Quality Assurance

The customer-identified functional classification for these tasks is Safety Class.[8-9] Requirements for performing reviews of technical reports and the extent of review are established in Manual E7 2.60.[33] This document, including all calculations (e.g., hydrogen generation rates and uncertainties), was reviewed by Design Verification by Document Review. SRNL documents the extent and type of review using the SRNL Technical Report Design Checklist contained in WSRC-IM-2002-00011, Rev. 2.[34] Data are recorded in the electronic laboratory notebook system as notebook/experiment numbers A6583-00142-25 and 26, and other associated notebooks/experiments. Measurements, calculations, documentation, and technical review comply with the customer required quality assurance level to support Safety Class use of information contained in this report.

For the flow system, the DAC software package used to control, display, and log test parameters is software classification level D.[35] The DAC software controls the heating, mixing, and gas purge flow; displays the test measurements to the user; and records a data file for later use. The DAC software does not perform calculations that are used in this report. The logged data that contributes to HGR calculations are the purge gas flows and the reaction temperature. The purge gas flow instruments, thermocouples, and temperature scanner are in the Measuring and Test Equipment (M&TE) program. Each of these instruments has an alternative reading outside of the DAC software. Data is periodically recorded manually (e.g., every 30 minutes) to supplement the files generated by the DAC software.

As described previously, two commercially available statistical software packages (GUM Workbench and JMP® Pro) are utilized for uncertainty analyses for HGR measurements. For these packages, the software classification is level D.[36-37] Both statistical packages have undergone verification and validation.[38] Calculations performed by these software packages are subjected to the technical review process.

Analytical measurements for gas streams were made with GCs. The GCs are in the Measurement Systems and Equipment (MS&E) program and thus their software is controlled under the requirements of the MS&E program. The reprocessed data from the GC software is used in the HGR calculations.

3.0 Samples and Analysis

The Tank 39 3-L sample HTF-39-19-1 was received at SRNL on January 16, 2019. The Tank 28 3-L sample FTF-28-19-8 was received at SRNL on April 4, 2019. These two samples were used in the HGR testing reported in this document. Figure 3-1 contains photographs of the Tank 28 and Tank 39 samples in one-gallon glass jars taken upon removal from the samplers. The Tank 28 and Tank 39 samples contained approximately 4574 g and 3873 g of material, respectively. The Tank 28 sample was mostly clear but appeared dark through the cell window because it had a blue/violet hue. The Tank 28 material had a few large clear salt crystals that were evident in the sampler and the transfer tubing. The Tank 39 sample was slightly cloudy and appeared light brown. The Tank 39 supernate was pale yellow but contained a small amount (which was not quantified but was likely approximately 0.1 wt %) of brown insoluble solids that settled in about one day. The solids contained in the Tank 39 sample were split among sub-samples and thus were present in the HGR testing.

Table 3-1 and Table 3-2 contain the analytical data related to the Tank 28 and Tank 39 HGR tests, respectively. Averages and relative standard deviations (RSD) of duplicate measurements are reported. Results are preceded by "<" when the analyte is below the LOQ. LOQs for additional non-detected analytes are contained in Appendix B.

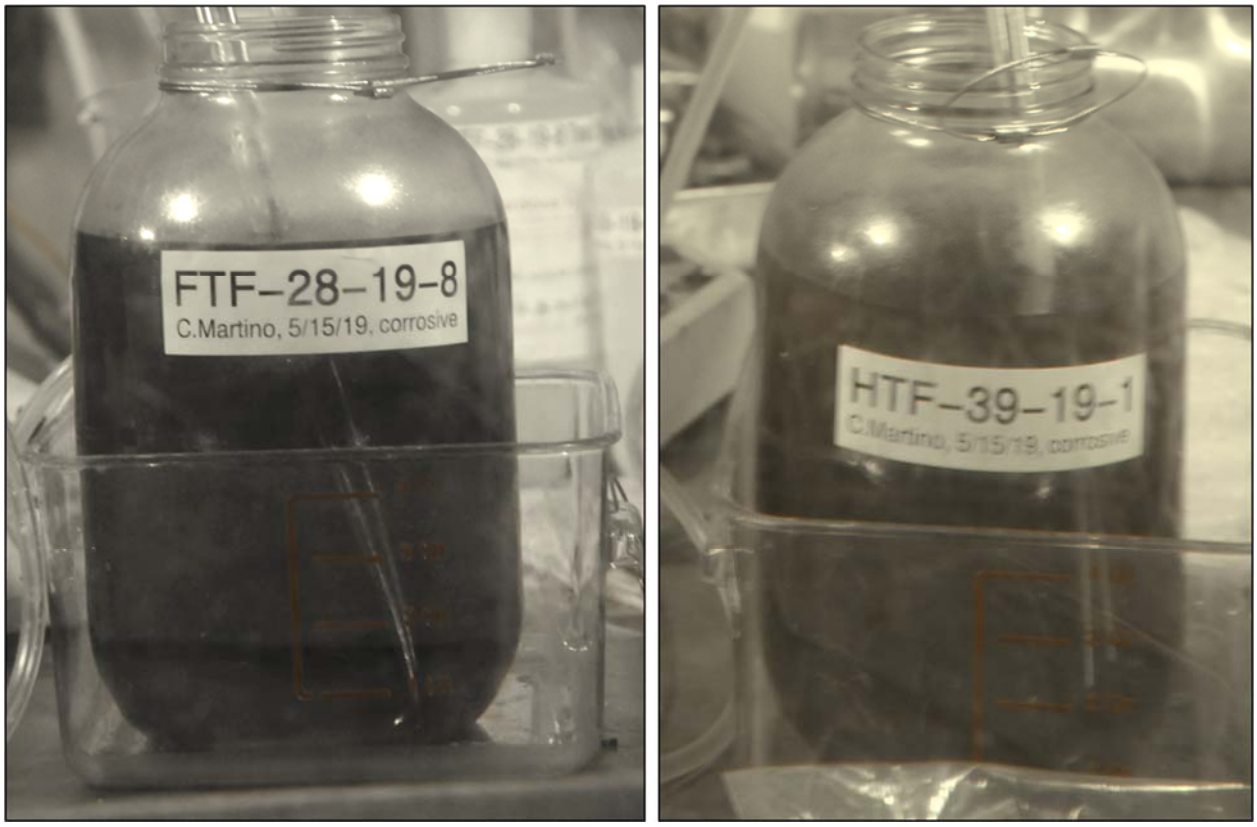

Figure 3-1. Tank 28 sample FTF-28-19-8 (left) and Tank 39 sample HTF-39-19-1 (right)

The columns labeled "Feed" in the tests without glycolate contains the analysis of the as-received tank samples and thus received the most extensive analysis. The columns labeled "Feed" in the tests with added glycolate are the results for the sample taken after the 70 °C conditions of the tests with added glycolate. Those glycolate-test feeds received limited characterization, with the primary goal of measuring glycolate and TOC. The other analytes for the test feed without glycolate should apply to the test with added glycolate as well. The columns labelled "Post HGR" contain the samples of the sample material after use in the HGR tests.

As seen in Table 3-1, Tank 28 is a concentrated salt supernate with overall high sodium (13.0 M) and hydroxide (8.2 M) concentrations and a density of 1.462 g/mL. The other major salt anions are nitrite (2.0 M), nitrate (1.85 M), and aluminate (0.76 M). Testing of post-HGR samples yielded slightly different anion and cation concentrations from the feed. The TOC concentration for the Tank 28 sample test without glycolate was 531 mg/L (Relative Standard Deviation, RSD = 12%) in the feed and 195 mg/L (RSD = 11%) in the product. The change in TOC from before to after the HGR measurement implies significant destruction of organics in the Tank 28 material due to heating. Formate, oxalate, sulfate, and mercury were below the limit of detection. For the Tank 28 HGR test with 500 mg/L of added glycolate, the feed measured 438 mg/L glycolate and the post-HGR sample measured 479 mg/L glycolate. Comparing masses and densities of the sample before and after HGR testing, the glycolate concentration difference between the feed and the post-HGR sample measurements was not due to evaporation of the sample.

Analysis of liquid associated with a previous Tank 28 sample saltcake (FTF-456 thorough 467, received in 2006) had a measured TOC of 4020 mg/L.[21] Considering the formate in the sample, the net unknown TOC was 3940 mg/L. A reanalysis of this same Tank 28 liquid material from FTF-456 thorough 467 was performed in April 2019, after over 12 years in storage, with a measured TOC of 170 mg/L. Considering

the formate in the sample, the net unknown TOC in April 2019 was 120 mg/L. The current Tank 28 supernate sample FTF-28-19-8 measured 531 mg/L TOC, with formate below the detectable level. The previous measurements of higher TOC in Tank 28 may have been due to a high bias in TOC measurements. In approximately 2008, SRNL measurement system for TOC was changed from a method that calculated TOC based on a difference between Total Carbon (TC) and TIC measurements to a method that converts TOC to CO_2 and provides a more direct TOC measurement.

The current TOC measurement system is much less susceptible to high bias due to high sample TIC or incomplete TIC conversion. In the current Tank 28 sample analysis, several relative TOC measurements are not consistent with expectation. For example, TOC in the feed without glycolate is greater than TOC in the feed with glycolate. Also, TOC in the feed with glycolate is less than TOC in the post-HGR sample with glycolate. Use of these TOC data is difficult due to these anomalies.

As seen in Table 3-2, Tank 39 is a moderately concentrated salt supernate with sodium of 5.55 M, nitrate of 2.2 M, and hydroxide of 1.8 M. Nitrite (0.25 M), carbonate (0.2 M), aluminate (0.2 M), and sulfate (0.04 M) were also noted. The TOC concentration for the Tank 39 sample test without glycolate was 236 mg/L (RSD = 1.4%) in the feed and 94 mg/L (RSD = 22%) in the product. Formate and oxalate were below the limit of detection. For the Tank 39 HGR test with 2000 mg/L of added glycolate, the feed measured 2020 mg/L glycolate and the post-HGR sample measured 1960 mg/L glycolate.

Table 3-1. Analysis of Tank 28 feed sample (FTF-28-19-8) and post-HGR test sample analysis

analyte	method	units	Tank 28 without glycolate				Tank 28 with 500 mg/L glycolate			
			Feed		Post HGR		Feed		Post HGR	
			average	RSD	average	RSD	average	RSD	average	RSD
density	gravimetric	g/mL	1.462	0.10%	n.d.	--	n.d.	--	n.d.	--
Na^+	ICP-ES	M	1.30E+01	4.2%	1.43E+01	2.4%	n.d.	--	1.46E+01	20%
OH^-	titration	M	8.23E+00	0.8%	8.11E+00	4.4%	n.d.	--	8.05E+00	3.3%
NO_3^-	IC	M	1.85E+00	20%	1.53E+00	2.0%	1.41E+00	17%	1.54E+00	0.7%
NO_2^-	IC	M	1.99E+00	19%	1.70E+00	0.6%	1.53E+00	18%	1.64E+00	1.4%
CO_3^{2-}	TIC/TOC	M	7.62E-02	4.1%	6.99E-02	1.8%	6.14E-02	0.2%	1.20E-01	3.0%
$Al(OH)_4^-$	ICP-ES	M	7.60E-01	3.3%	7.69E-01	1.3%	n.d.	--	7.67E-01	3.7%
SO_4^{2-}	IC	M	<1.5E-03	--	<3.7E-02	--	<1.1E-02	--	<1.9E-02	--
PO_4^{3-}	IC	M	2.07E-02	22%	<3.8E-02	--	<1.1E-02	--	<1.9E-02	--
Cl^-	IC	M	2.32E-02	14%	<1.0E-01	--	<3.0E-02	--	<5.1E-02	--
CHO_2^-	IC	M	<3.2E-03	--	<8.0E-02	--	<2.4E-02	--	<4.0E-02	--
$C_2O_4^{2-}$	IC	M	<2.6E-03	--	<4.1E-02	--	<1.2E-02	--	<2.1E-02	--
$C_2H_3O_3^{2-}$	IC	M	n.d.	--	n.d.	--	5.84E-03	0.7%	6.39E-03	0.5%
		mg/L					4.38E+02		4.79E+02	
TOC	TIC/TOC	mg C/L	5.31E+02	12%	1.95E+02	11%	3.34E+02	0.3%	5.58E+02	1.8%
Hg	DMA	mg/L	<3.7E-01	--	n.d.	--	n.d.	--	n.d.	--
B	ICP-ES	mg/L	9.90E+01	0.5%	9.54E+01	2.5%	n.d.	--	9.44E+01	3.5%
Ca	ICP-ES	mg/L	<7.4E+00	--	7.84E+00	2.9%	n.d.	--	<7.2E+00	--
Cr	ICP-ES	mg/L	1.73E+02	3.7%	1.72E+02	3.0%	n.d.	--	1.72E+02	2.1%
Fe	ICP-ES	mg/L	2.22E+01	1.1%	2.30E+01	3.1%	n.d.	--	2.48E+01	11%
K	ICP-ES	mg/L	5.68E+03	3.5%	5.89E+03	2.1%	n.d.	--	5.99E+03	1.4%
Mo	ICP-ES	mg/L	1.05E+02	4.0%	1.02E+02	3.9%	n.d.	--	1.06E+02	2.3%
P	ICP-ES	mg/L	9.14E+02	3.1%	9.01E+02	4.2%	n.d.	--	8.94E+02	3.2%
S	ICP-ES	mg/L	5.33E+02	6.2%	<6.3E+02	--	n.d.	--	5.04E+02	5.6%
Si	ICP-ES	mg/L	3.40E+01	1.3%	<3.8E+01	--	n.d.	--	3.30E+01	0.8%
Zn	ICP-ES	mg/L	2.66E+01	4.4%	2.72E+01	4.4%	n.d.	--	2.85E+01	0.3%
Tc-99	ICP-MS	mg/L	1.17E+01	1.0%	n.d.	--	n.d.	--	n.d.	--
		pCi/mL	1.99E+05							
Cs-137	gamma	dpm/mL	2.00E+09	0.9%	n.d.	--	n.d.	--	n.d.	--
Ba-137m			1.89E+09							
U-235	ICP-MS	mg/L	<3.7E-02	--	n.d.	--	n.d.	--	n.d.	--
U-238	ICP-MS	mg/L	8.03E-01	6.4%	n.d.	--	n.d.	--	n.d.	--

n.d. – not determined

Table 3-2. Analysis of Tank 39 feed sample (HTF-39-19-1) and post-HGR test sample analysis

analyte	method	units	Tank 39 without glycolate				Tank 39 with 2 g/L glycolate			
			Feed		Post HGR		Feed		Post HGR	
			average	RSD	average	RSD	average	RSD	average	RSD
density	gravimetric	g/mL	1.235	0.02%	n.d.	--	n.d.	--	n.d.	--
Na^+	ICP-ES	M	5.55E+00	11%	5.08E+00	1.8%	n.d.	--	5.82E+00	7.0%
OH^-	titration	M	1.79E+00	3.4%	1.74E+00	20.3%	n.d.	--	1.67E+00	16.0%
NO_3^-	IC	M	2.20E+00	3.7%	2.30E+00	1.3%	2.41E+00	13.9%	2.27E+00	0.5%
NO_2^-	IC	M	2.47E-01	5.5%	2.71E-01	3.8%	2.80E-01	14.8%	2.60E-01	9.2%
CO_3^{2-}	TIC/TOC	M	2.08E-01	1.5%	2.14E-01	0.6%	2.52E-01	0.5%	2.15E-01	1.7%
$Al(OH)_4^-$	ICP-ES	M	1.99E-01	3.5%	2.01E-01	1.7%	n.d.	--	2.11E-01	4.5%
SO_4^{2-}	IC	M	3.99E-02	2.4%	3.84E-02	0.9%	4.03E-02	13.6%	3.83E-02	3.4%
CHO_2^-	IC	M	<1.5E-03	--	<2.7E-02	--	<5.3E-02	--	<1.4E-02	--
$C_2O_4^{2-}$	IC	M	<1.2E-03	--	<1.4E-02	--	<2.7E-02	--	<7.3E-03	--
$C_2H_3O_3^{2-}$	IC	M	n.d.	--	n.d.	--	2.69E-02	4.2%	2.61E-02	0.1%
		mg/L					2.02E+03		1.96E+03	
TOC	TIC/TOC	mg C/L	2.36E+02	1.4%	9.44E+01	21.7%	8.50E+02	1.0%	7.30E+02	1.4%
Hg	DMA	mg/L	6.74E+01	1.4%	n.d.	--	n.d.	--	n.d.	--
B	ICP-ES	mg/L	7.87E+01	1.6%	7.45E+01	1.0%	n.d.	--	7.99E+01	5.7%
Ca	ICP-ES	mg/L	<6.1E+00	--	3.24E+00	15.0%	n.d.	--	<2.7E+00	--
Cr	ICP-ES	mg/L	1.18E+02	1.8%	1.13E+02	1.2%	n.d.	--	1.20E+02	5.6%
Fe	ICP-ES	mg/L	1.26E+01	12.3%	1.28E+01	4.9%	n.d.	--	7.37E+00	4.0%
K	ICP-ES	mg/L	2.99E+02	3.1%	2.84E+02	1.2%	n.d.	--	3.03E+02	5.2%
Mn	ICP-ES	mg/L	7.62E+00	11.2%	6.74E+00	6.9%	n.d.	--	<2.5E+00	--
Mo	ICP-ES	mg/L	<2.5E+01	--	2.42E+01	0.3%	n.d.	--	2.31E+01	9.2%
P	ICP-ES	mg/L	3.65E+01	8.6%	3.31E+01	2.2%	n.d.	--	<4.1E+01	--
S	ICP-ES	mg/L	1.62E+03	1.2%	1.64E+03	1.5%	n.d.	--	1.62E+03	4.9%
Si	ICP-ES	mg/L	1.96E+01	5.1%	1.79E+01	3.2%	n.d.	--	1.93E+01	6.1%
Tc-99	ICP-MS	mg/L	1.89E+00	0.1%	n.d.	--	n.d.	--	n.d.	--
		pCi/mL	3.20E+04							
Cs-137	gamma	dpm/mL	3.47E+08	0.2%	n.d.	--	n.d.	--	n.d.	--
Ba-137m			3.28E+08							
U-234	ICP-MS	mg/L	3.68E-02	2.7%	n.d.	--	n.d.	--	n.d.	--
U-235	ICP-MS	mg/L	9.91E-01	1.0%	n.d.	--	n.d.	--	n.d.	--
U-236	ICP-MS	mg/L	1.55E-01	1.3%	n.d.	--	n.d.	--	n.d.	--
U-238	ICP-MS	mg/L	8.30E+00	0.2%	n.d.	--	n.d.	--	n.d.	--
Np-237	ICP-MS	mg/L	3.54E-02	2.8%	n.d.	--	n.d.	--	n.d.	--
Pu-239	ICP-MS	mg/L	6.03E-02	8.3%	n.d.	--	n.d.	--	n.d.	--

n.d. – not determined

Table 3-3 contains the results of Tank 28 and Tank 39 sample measurements for methylmercury (MMHg) as well as for VOA and SVOA analytes. Several antifoam degradation products were analyzed for, including propanal, hexamethyldisiloxane (HMDSO), and trimethylsilanol (TMS). Most analytes were below the LOQ. Tank 28, which had total mercury below LOQ, also had MMHg below LOQ. MMHg in Tank 39 was 9.5 mg/L, or approximately 14% of the total mercury. Of the VOA and SVOA analytes, 0.12 mg/L of HMDSO was measured in the Tank 28 sample and 0.1 mg/L of unidentified VOA was measured in the Tank 39 sample.

Table 3-3. Tank 28 and Tank 39 feed analysis for methylmercury, VOA, and SVOA analytes

Analyte	Units	Tank 28	Tank 39
MMHg	mg/L	<1	9.5
propanal	mg/L	<0.1	<0.1
TMS	mg/L	<0.1	<0.1
HMDSO	mg/L	0.12	<0.1
VOA	mg/L	<0.1	0.1
SVOA	mg/L	<1.1	<1.1

4.0 HGR Test Results and Discussion

4.1 Results for Tank 28 Actual Waste without Added Glycolate

The full measurement profile including HGR, temperature, purge rates, and tracer measurements as a function of date and time is contained in Appendix C, Figure C-1.

4.1.1 Hydrogen Generation Rate Measurements

Table 4-1 and Figure 4-1 display tabulated and graphical results, respectively, for the Tank 28 sample HGR measurements without added glycolate. The measurements were performed in the following order: 70 °C (1st), 85 °C, 100 °C, 124.8 °C (boiling), 70 °C (2nd), and 40 °C (near-ambient). The measurement scheme differed from the planned progression of temperatures in two ways. First, a second 70 °C measurement was added after indications of the first 70 °C measurement and subsequent measurements led to a hypothesis that a second 70 °C measurement after the boiling condition would result in a lower HGR. Second, the final near-ambient 35 °C measurement was replaced with a near-ambient 40 °C measurement due to the high probability that either near-ambient condition would result in thermolytic HGR below the LOQ.

The first 70 °C HGR measurement showed a generally increasing trend that stabilized near 6.7×10^{-7} ft^3 h^{-1} gal^{-1}. Due to the short length of these tests, it is difficult to determine whether the first 70 °C HGR measurement was reaching a long-term stable value or a short-term maximum value. The subsequent measurements at 85 °C and 100 °C showed a decrease of approximately 6% per hour with no indication of trend in the decrease beyond noise. The average of the final nine HGR measurements (corresponding to the final 72 minutes of measurements) were approximately 6.1×10^{-7} ft^3 h^{-1} gal^{-1} at 85 °C and approximately 8.1×10^{-7} ft^3 h^{-1} gal^{-1} at 100 °C. The measurements for the 85 and 100 °C conditions are approximate because they are strongly influenced by the stopping point for each measurement condition due to the downward trends observed. The 95% confidence intervals (CI) in Table 4-1 capture the measurement instrument

uncertainties but do not capture the uncertainties associated with downward or upward trends during HGR measurement.

Increasing the temperature of the Tank 28 sample to the boiling point, 124.8 °C, yielded a thermolytic HGR increase to 6.27×10^{-6} ft^3 h^{-1} gal^{-1} (over final 15 measurements, final 2 hours) with a slight downward trend of less than 2% per hour. Due to the hysteresis evident in the 70, 85, and 100 °C HGR measurements, a second 70 °C HGR measurement was then performed. As expected, the second 70 °C measurement showed a notable decline to 1.3×10^{-7} ft^3 h^{-1} gal^{-1}. This second measurement appeared stable over the time of the measurement but exhibited more relative scatter due to approaching the LOQ. By comparison, the second measurement at 70 °C was only 19% of the first measurement at 70 °C, which was taken before submitting the sample to higher temperature measurements. This reduction in HGR is likely due to depletion of a portion of the organics that are contributing to thermolytic HGR in the first several measurement conditions.

Table 4-1. HGR measurements for Tank 28 sample without glycolate

T (°C)	HGR (ft^3 h^{-1} gal^{-1})	95% CI
40	<5.9E-08	--
70, 1st	6.7E-07	± 6.1%
70, 2nd	1.3E-07	± 6.1%
85	6.1E-07	± 5.3%
100	8.1E-07	± 5.3%
124.8	6.27E-06	± 5.3%

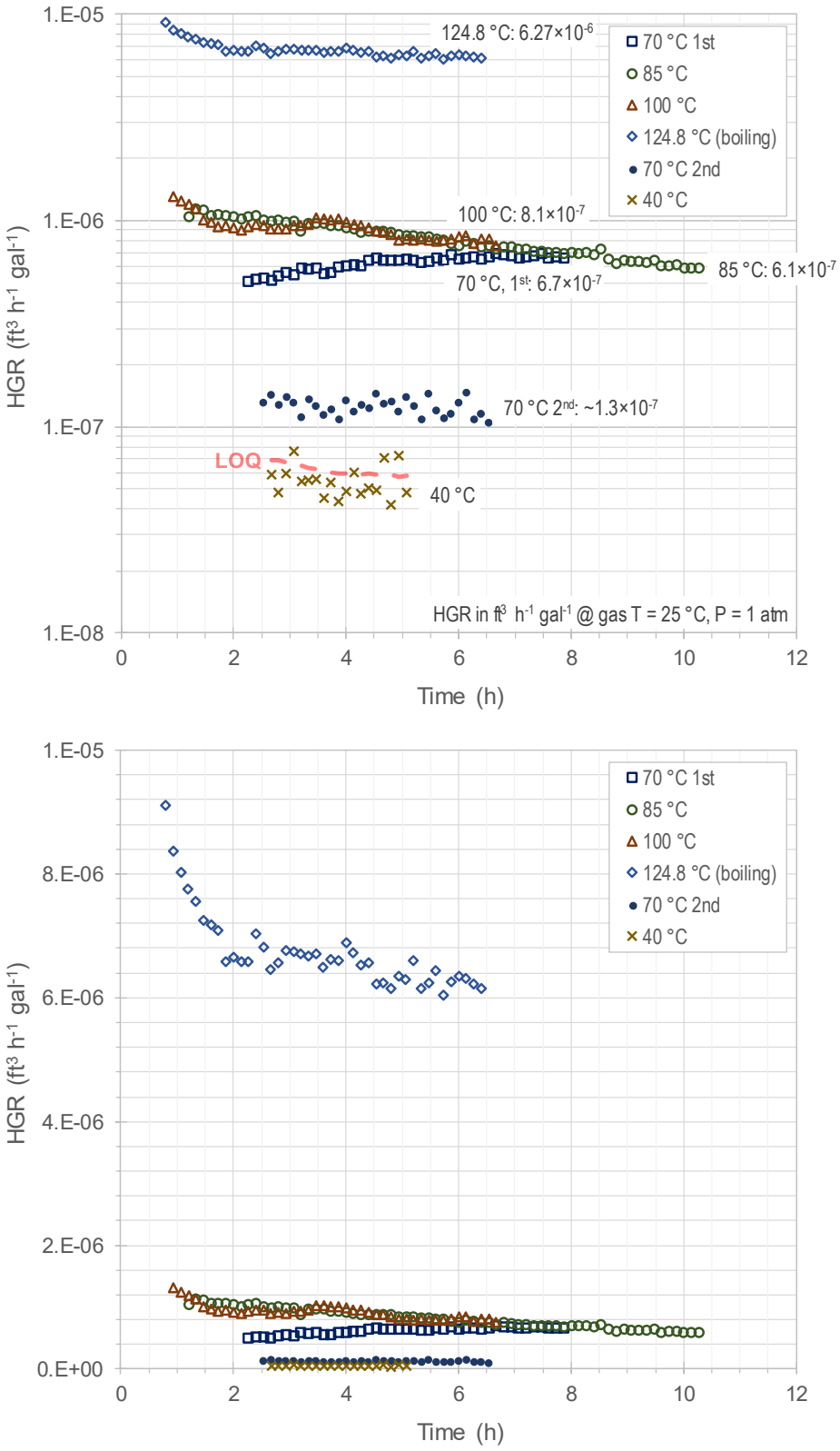

Figure 4-1. HGR measurements for Tank 28 sample without glycolate at a series of temperatures, logarithmic (top) and linear (bottom) scales

Finally, the HGR measurement of the Tank 28 sample at 40 °C was below the LOQ of 5.9×10^{-8} ft^3 h^{-1} gal^{-1}. Thus, HGR due to radiolysis was not able to be quantified for the Tank 28 sample during this test.

In Figure 4-1, the data reported for each test starts when $Kr/Kr_0 \geq 0.8$, which corresponds to between one and two vessel headspace turn-overs. The earliest time that measurements were concluded was the time required for three vessel headspace turn-overs plus allowing the time for air to reach the GC, which will total approximately 3.5 hours for the test conditions. Tests at most temperatures were extended slightly to allow for time for the trend in hydrogen concentration to stabilize. Time zero on Figure 4-1 corresponds to the time that the target temperature was attained. As seen in Appendix A, for each test, the measurements were performed for a series of temperatures on the same sample aliquot. The LOQ value is adjusted for Kr/Kr_0. Although the LOQ for hydrogen concentration is constant, the LOQ for HGR decreases with testing time as Kr/Kr_0 increases toward one. The 95% CI in Table 4-1 is based on the error propagation in the measurements, purge flows and gas concentrations evident in Equation 1. The HGR results at several of the temperatures showed decreasing trends with measurement time. Thus, some of the HGR results may contain additional bias not represented by the reported CI. As mentioned in Section 2.3.1, drift in the GC calibration for hydrogen and krypton was noted during this testing. The lowest applicable set of hydrogen areas and the highest applicable set of krypton areas were used in the HGR calculations of Equation 1. Thus, the calibration drift is included in a positive (i.e., conservative or high) bias in the HGR measurements rather than being factored into the CI.

Over the first three measurements of 70, 85, and 100 °C, there is not a strong temperature dependence of HGR. This alone could indicate that the hydrogen generation was by a means other than thermolysis. However, with the decreases noted while holding the tank sample solution at each temperature and the differences between the first and second 70 °C measurements, a better explanation of this lack of temperature dependence is either the depletion in the quantity of organics active toward thermolytic hydrogen generation or the release of dissolved hydrogen. From the Arrhenius plot given in Figure 4-2, the non-temperature dependent trend of the initial measurements was ignored.

The trend in the conditions of 100 °C to boiling at 124.8 °C to the second measurement at 70 °C was used to determine an activation energy (E_a) of approximately 80 kJ/mol. The 35 °C measurement was below the LOQ and thus was also not applicable in determination of the E_a.

At this time, it is unclear if the decrease observed in HGR over the full course of the Tank 28 experiment and the apparent temperature independence of the first three HGRs observed (70, 85, and 100 °C) is due to the presence of organic compounds that are rapidly destroyed upon heating, release of dissolved hydrogen gas, or some other hitherto unknown gas generation mechanism. It should be noted that the lack of temperature dependence over the variation of 30 °C is consistent with the behavior or mass-transport limited gas release, such as that observed during gas dissolution. However, given that these phenomena are apparently transient and dissipate over the course of the full experiment, it is not expected that these initially "high" observed HGRs are representative of waste tanks generating hydrogen over the course of days and months. Furthermore, such transients would be expected to dissipate within a single pass through an evaporator system and should not be considered relevant to long-term flammability considerations in evaporator-system waste tanks.

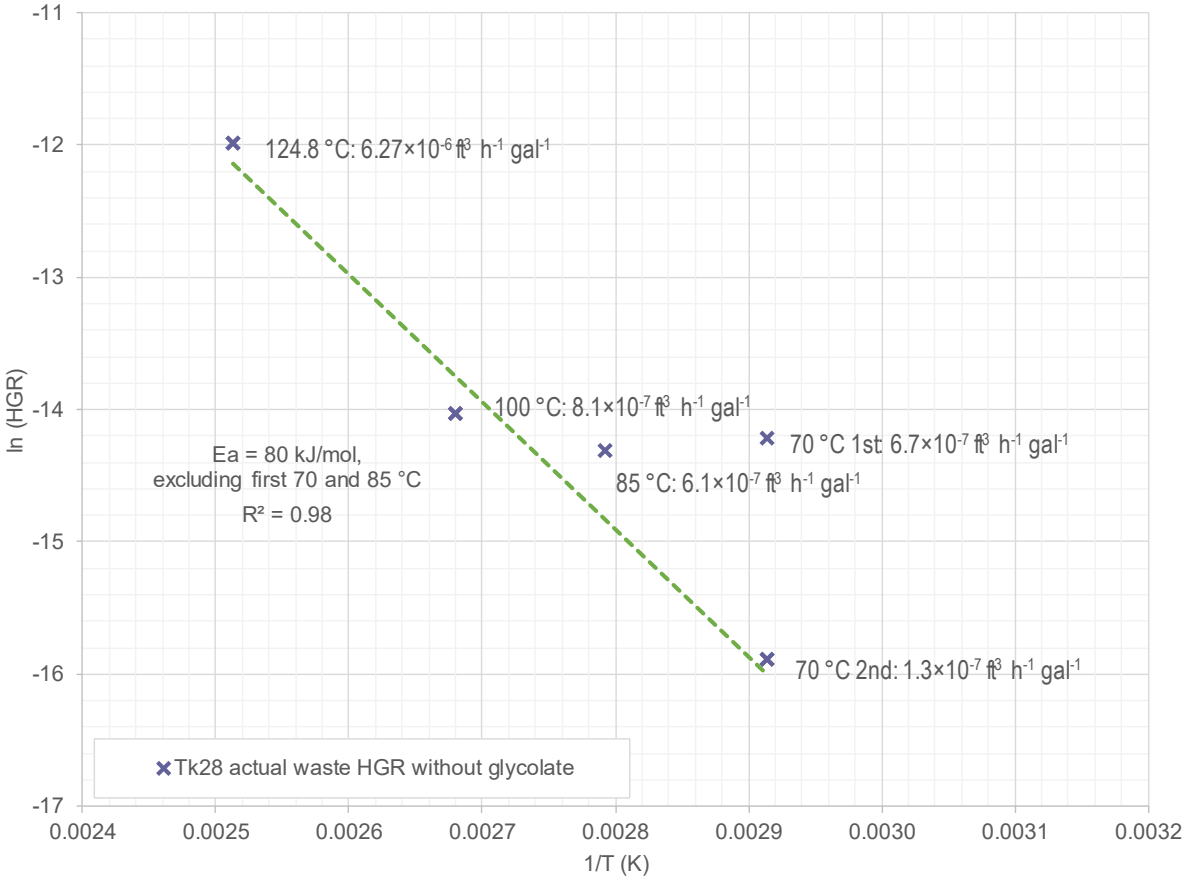

Figure 4-2. Arrhenius plot for hydrogen generation of Tank 28 sample without glycolate

4.1.2 Other Gas Generation

Methane, nitrous oxide, and carbon dioxide were measured in the offgas stream during portions of Tank 28 sample HGR measurements without added glycolate.

Methane was only seen at the boiling condition (124.8 °C) during Tank 28 sample testing. Figure 4-3 contains a comparison of methane concentration to hydrogen concentration during Tank 28 sample boiling. Methane was only seen at levels up to near its LOQ of 14 ppmv; and methane was present at approximately 1/10 the concentration of hydrogen at the end of the test condition. At the purge rate of 5.4 mL/min used in this testing, the 14 ppmv LOQ for methane corresponds to approximately 5.7×10^{-7} ft^3 h^{-1} gal^{-1}.

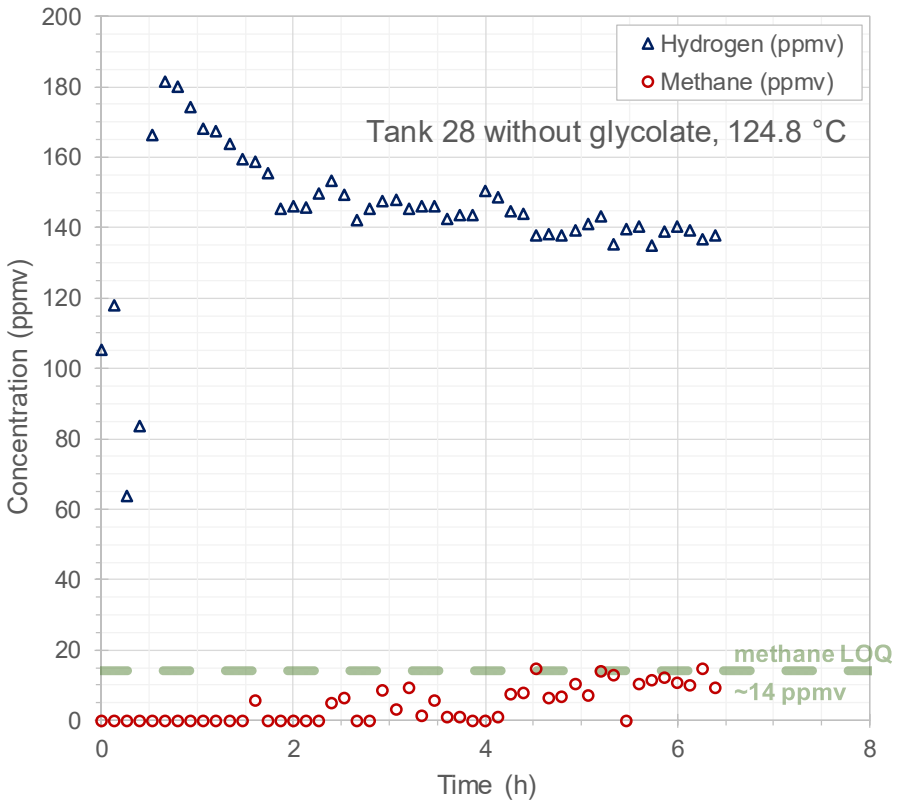

Figure 4-3. Methane and hydrogen concentration from the at boiling condition (124.8 °C) of the Tank 28 sample HGR test without added glycolate

Carbon dioxide and nitrous oxide data can be seen in Appendix D. Carbon dioxide was measured at approximately 0.002 to 0.005 mol %. The different purge rates used for different temperature conditions partially masks a slight inverse temperature dependence in carbon dioxide measurements. Nitrous oxide concentration measurements displayed an increase with increasing temperature (when adjusted for purge rate) up to the boiling condition. At the boiling condition, nitrous oxide concentration showed a sharp peak to around 0.08 vol % when boiling was achieved followed by a drop-off to around 0.013 vol % at the end of the HGR measurement condition. The initial nitrous oxide peak at boiling occurs during a period in the HGR test where quantitative rate data cannot be determined due to the changes in the test purge and the apparent temporary nature of the release. The reduction in nitrous oxide concentration during the boiling test condition was much more pronounced than the change in hydrogen concentration during the same period. After the boiling condition, the second 70 °C HGR measurement condition was below detection for nitrous oxide. This contrast between the approximately 0.005 mol % nitrous oxide during the first 70 °C measurement and the below detection result for nitrous oxide during the second 70 °C measurement indicates that processing this stream at increased temperature lowers the future release of nitrous oxide at lower temperatures. This phenomenon is consistent with both the release of a soluble gas and the reduction in generation potential of the gas.

4.2 Results for Tank 28 Waste with Added Glycolate

The full measurement profile including HGR, temperature, purge rates, and tracer measurements as a function of date and time is contained in Appendix C, Figure C-4.

4.2.1 Hydrogen Generation Rate Measurements

Table 4-2 and Figure 4-4 display tabulated and graphical results, respectively, for the Tank 28 sample HGR measurements with 500 mg/L of added glycolate. The measurements were performed in the following order: 70 °C, 85 °C, 100 °C, 124.8 °C (boiling), and 35 °C (near-ambient).

The 70 °C HGR measurement showed a generally increasing trend that stabilized near 1.42×10^{-6} ft^3 h^{-1} gal^{-1}. This 70 °C HGR measurement with 500 mg/L added glycolate was roughly double of the 70 °C HGR measurement without glycolate of 6.7×10^{-7} ft^3 h^{-1} gal^{-1}. For the subsequent measurements, the 85 °C HGR measurement stabilized relatively quickly to an HGR of 3.02×10^{-6} ft^3 h^{-1} gal^{-1} and the 100 °C measurement increased over a 10 hour period where it then held relatively steady for six hours with an HGR of 1.17×10^{-5} ft^3 h^{-1} gal^{-1}. Increasing the temperature of the Tank 28 sample to the boiling point, 124.8 °C, the thermolytic HGR increased to 1.42×10^{-4} ft^3 h^{-1} gal^{-1} with a slight downward trend of approximately 3% per hour. Subsequent cooling and measurement at 35 °C resulted in an HGR of 3.0×10^{-7} ft^3 h^{-1} gal^{-1}. The time over which measurements were averaged for each condition was 72 minutes for 35 °C, 2 hours for 70, 85, and 124.8 °C, and 6 hours for 100 °C.

Since a previously unheated aliquot of Tank 28 sample was used in this HGR testing, the HGR measurements contains a known contribution to thermolytic and radiolytic HGR from the sample itself in addition to the thermolytic HGR from glycolate. The contribution of the thermolytic HGR due to glycolate may be calculated by subtracting the HGR measurements for the test without added glycolate from the HGR measurements for the test with added glycolate. In addition to the as-measured HGR from the Tank 28 test with 500 mg/L added glycolate, Table 4-2 also contains values for the HGR adjusted to reflect the contribution exclusively due to the added glycolate. Note that the 95% C.I. values displayed in Table 4-2 are only applicable to the as-measured HGR.

Table 4-2. HGR measurements for Tank 28 sample with 500 mg/L of added glycolate

T (°C)	HGR (ft^3 h^{-1} gal^{-1})		95% CI
	as measured[a]	adjusted[b]	
35	3.0E-07	--	± 6.4%
70	1.42E-06	7.5E-07	± 6.4%
85	3.02E-06	2.41E-06	± 6.4%
100	1.17E-05	1.09E-05	± 5.4%
124.8	1.42E-04	1.35E-04	± 5.4%

[a] as-measured HGR includes both glycolate and non-glycolate related hydrogen generation
[b] adjusted HGR subtracts non-glycolate related HGR from the as-measured HGR to yield glycolate thermolysis HGR

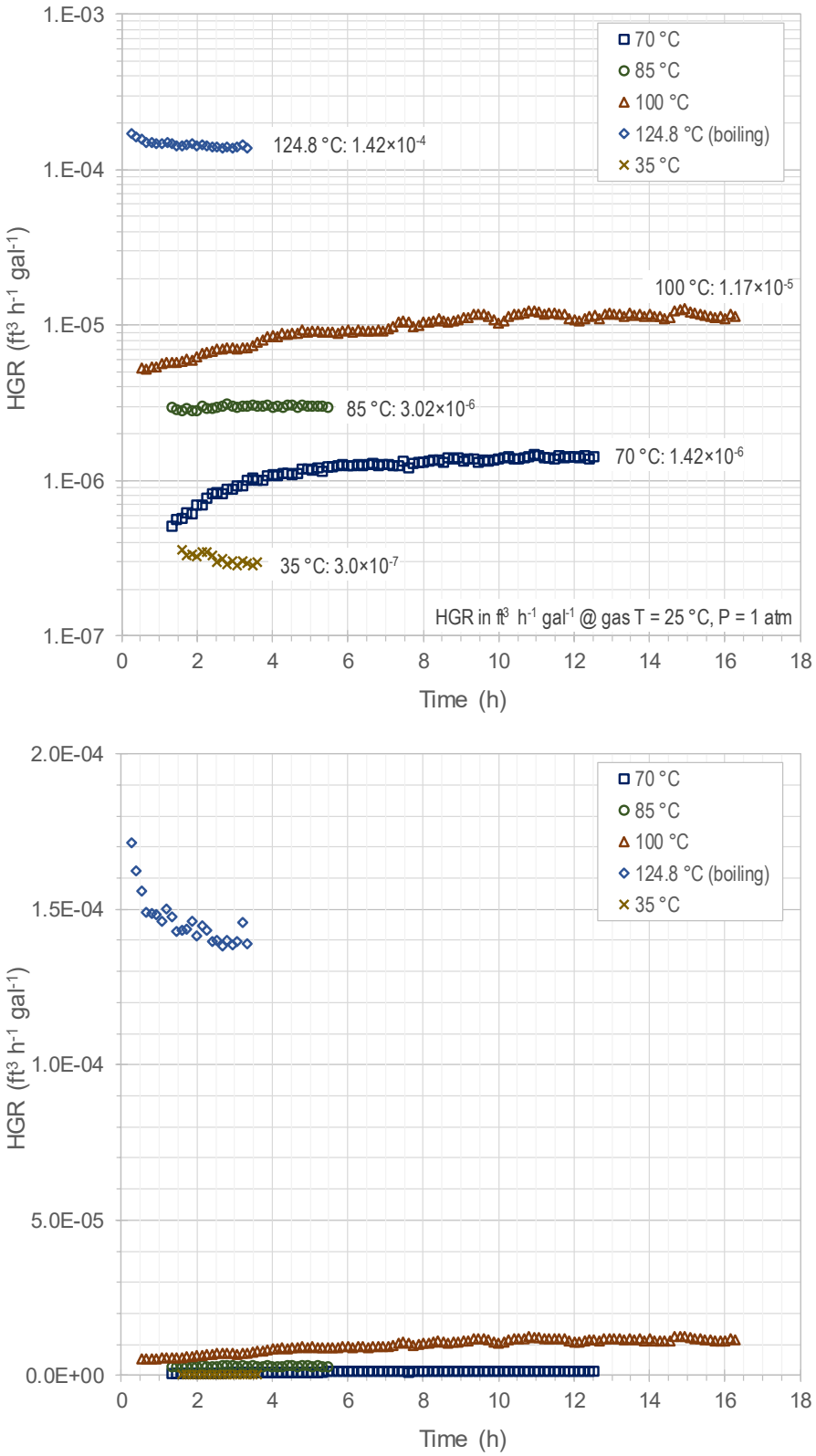

Figure 4-4. HGR measurements for Tank 28 sample with 500 mg/L of added glycolate at a series of temperatures, logarithmic (top) and linear (bottom) scales

Figure 4-5 contains the Arrhenius plot of the as-measured HGR for the Tank 28 sample with 500 mg/L of added glycolate. The linearity of the plot appeared to show a strong temperature dependence for the high temperature data, but the relationship did not appear to extend linearly to the lower temperatures. This is consistent with the knowledge that multiple hydrogen-generating reactions are proceeding in the reaction mixture across this range. Furthermore, the non-linear behavior suggests that the HGR observed at higher temperatures is dominated by the thermolytic production of hydrogen from glycolate. The activation energy (E_a) for the higher temperatures (85 to 124.8 °C) had an apparent value of 115 kJ/mol.

As seen in Figure 4-6, which uses the adjusted HGR to isolate the contribution of glycolate on the observed HGR, the Arrhenius plot appeared relatively linear for temperatures from 70 to 124.8 °C and had an apparent E_a of 108 kJ/mol.

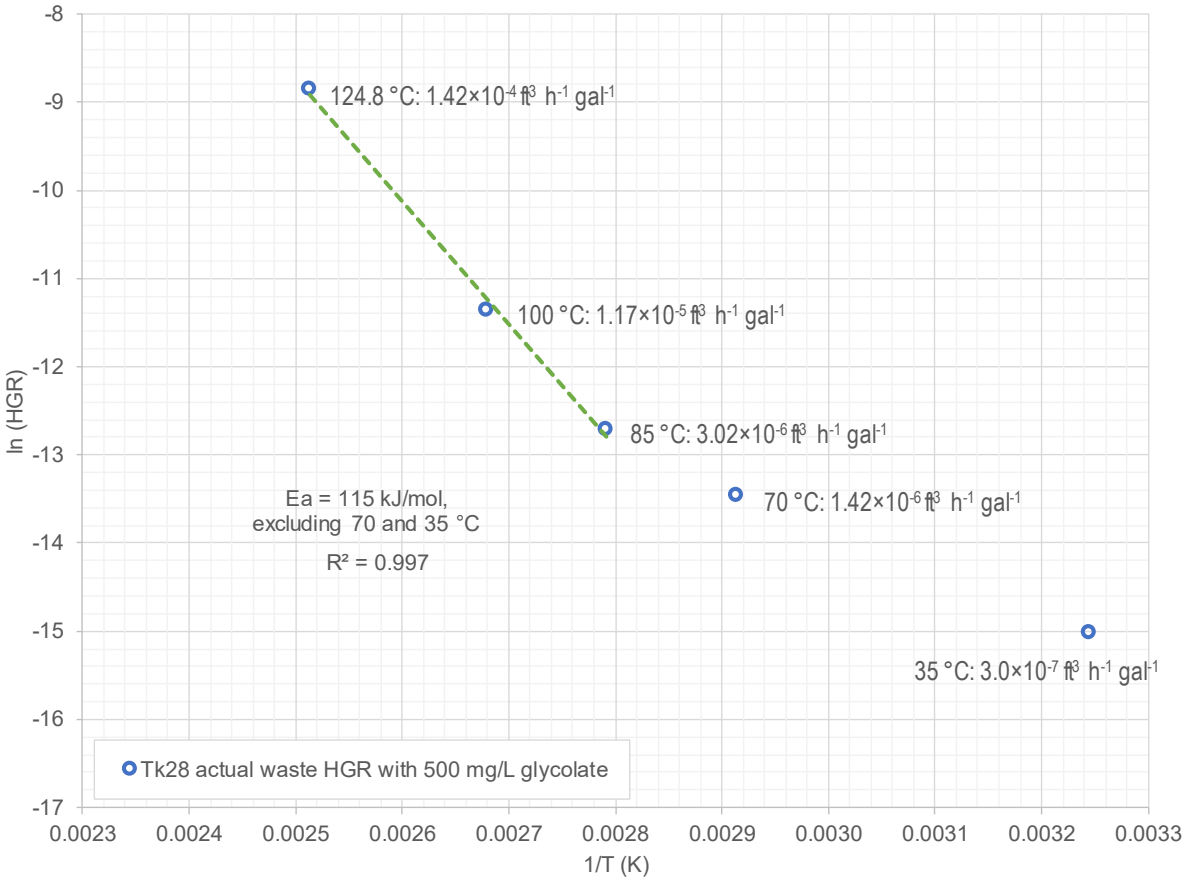

Figure 4-5. Arrhenius plot for hydrogen generation of Tank 28 sample with 500 mg/L of added glycolate

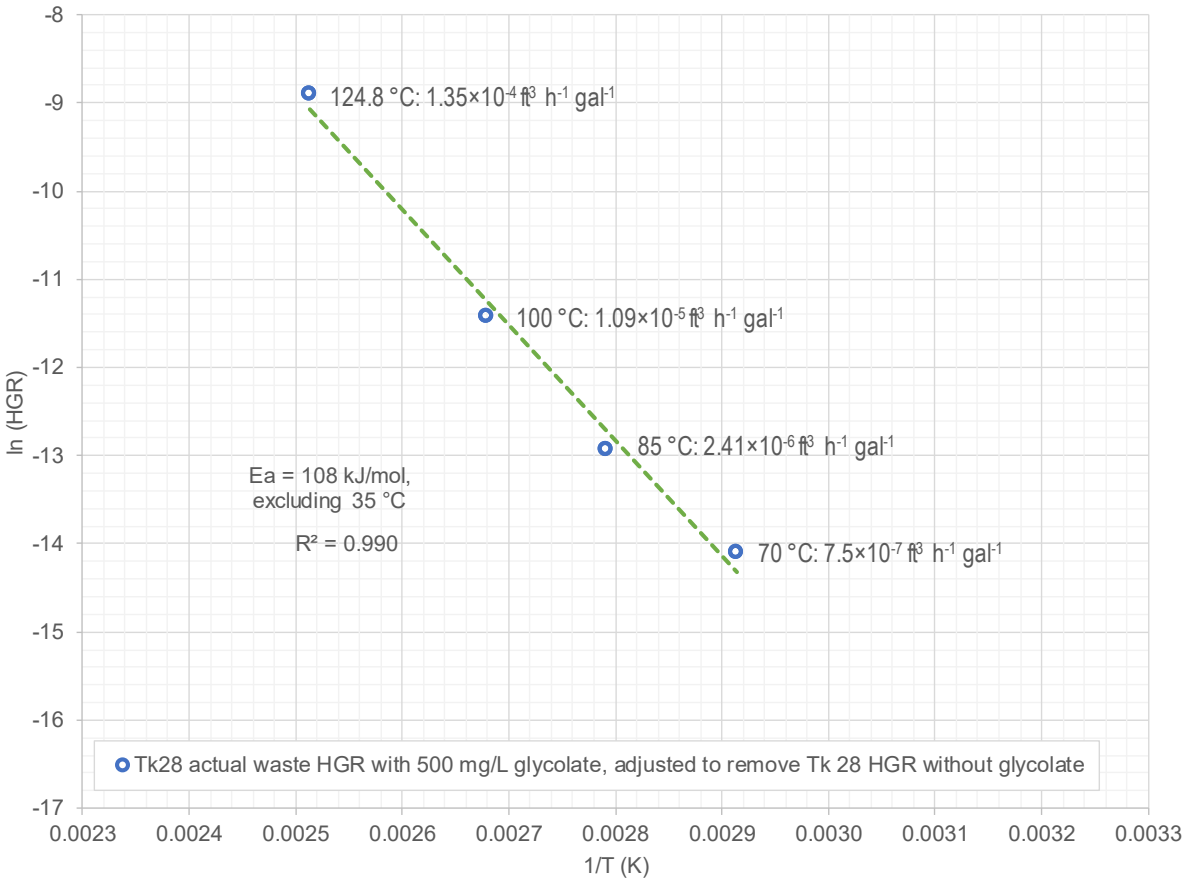

Figure 4-6. Arrhenius plot for hydrogen generation of Tank 28 sample with 500 mg/L of added glycolate, adjusted to remove the contribution of the Tank 28 sample without glycolate

4.2.2 Other Gas Generation

Methane was not generated at detectable levels during Tank 28 sample HGR measurements with 500 mg/L of added glycolate over the full temperature range. At the purge rate of 10 mL/min used in for the boiling condition, the 14 ppmv LOQ for methane corresponds to approximately 1.1×10^{-6} ft^3 h^{-1} gal^{-1}. Carbon dioxide and nitrous oxide data can be seen in Appendix D. Carbon dioxide and nitrous oxide measurements showed similar trends to the Tank 28 HGR test offgas measurements without added glycolate, as seen in Section 4.1.2. Nitrous oxide was most apparent at 100 °C and boiling, where it again exhibited a sharp peak at the onset of boiling. Carbon dioxide was below the detection limit at the 100 °C and boiling conditions. The increased purge in this test (5 to 10 mL/min) versus the Tank 28 test without glycolate (3 to 5.4 mL/min) is the primary reason for lower nitrous oxide and carbon dioxide concentration measurements in these tests. Adjusting for the purge rate, the nitrous oxide and carbon dioxide release behavior appears comparable to the Tank 28 test without added glycolate.

4.3 Results for Tank 39 Actual Waste without Added Glycolate

The full measurement profile including HGR, temperature, purge rates, and tracer measurements as a function of date and time is contained in Appendix C, Figure C-2.

4.3.1 Hydrogen Generation Rate Measurements

Table 4-3 and Figure 4-7 display tabulated and graphical results, respectively, for the Tank 39 sample HGR measurements without added glycolate. The measurements were performed in the following order: 70 °C, 85 °C, 100 °C, 105.3 °C (boiling), and 34.6 °C (near-ambient).

The 70, 85, and 100 °C HGR measurement all showed decreasing trends in HGR while holding at temperature. The HGR measurements also did not exhibit strong dependence on temperature. The HGR measurements at these conditions should be considered approximate because they are strongly influenced by the stopping point for each measurement condition due to the downward trends observed. The 95% CIs are not provided for HGR measurements at and below 100 °C in Table 4-3 because the CI values would be misleading.[b] The HGR measurement at the boiling condition of 105.3 °C yielded a somewhat scattered set of data that did not have an apparent decreasing or increasing trend. Averaging the final 2 hours of measurements, the HGR for the Tank 39 sample at the boiling condition of 105.3 °C was 1.4×10^{-7} ft^3 h^{-1} gal^{-1}. Subsequent cooling and HGR measurement of the Tank 39 sample at 34.6 °C was below the LOQ of 5.5×10^{-8} ft^3 h^{-1} gal^{-1}. Thus, HGR due to radiolysis was not able to be quantified for the Tank 39 sample during this test.

An Arrhenius plot is not given for this case and an activation energy was not calculated.

Table 4-3. HGR measurements for Tank 39 sample without glycolate

T (°C)	HGR (ft^3 h^{-1} gal^{-1})	95% CI
34.6	<5.5E-08	--
70	7E-08	--
85	7E-08	--
100	8E-08	--
105.3	1.4E-07	± 6.1%

[b] The calculated 95% CI values are not applicable for HGR measurements below the LOQ and for HGR measurements that have not attained a quasi-steady state and have decreased to near the LOQ.

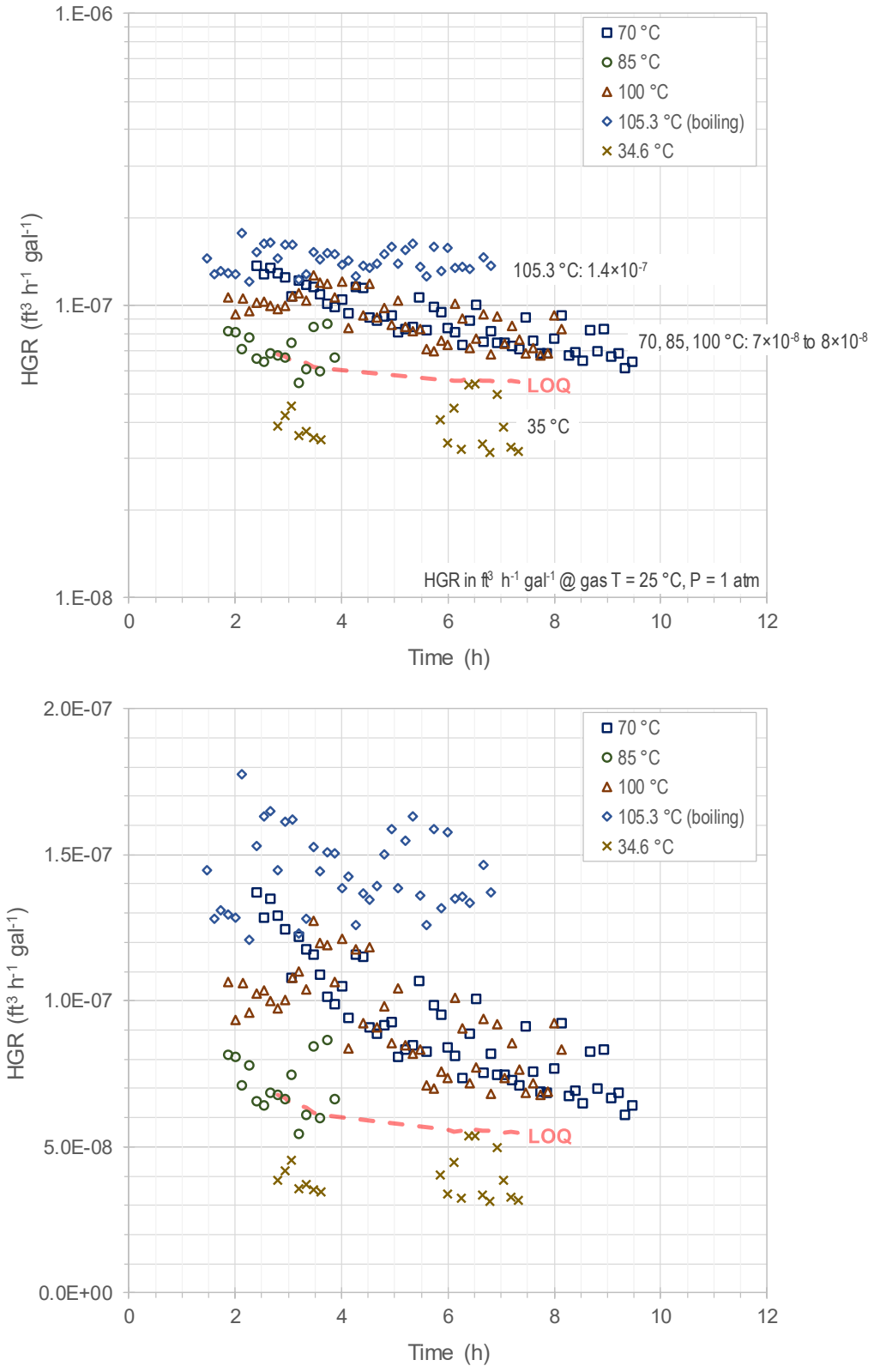

Figure 4-7. HGR measurements for Tank 39 sample without glycolate at a series of temperatures, logarithmic (top) and linear (bottom) scales

4.3.2 Other Gas Generation

Neither methane nor nitrous oxide were generated at detectable levels during Tank 39 sample HGR measurements without added glycolate over the full temperature range. The 3 mL/min purge rate used during this testing would have allowed for the greatest chance of detecting these gasses. Carbon dioxide was measured at approximately 0.003 to 0.005 mol % and had a slight inverse temperature dependence. Carbon dioxide data can be seen in Appendix D.

4.4 Results for Tank 39 Waste with Added Glycolate

The full measurement profile including HGR, temperature, purge rates, and tracer measurements as a function of date and time is contained in Appendix C, Figure C-3.

4.4.1 Hydrogen Generation Rate Measurements

Table 4-4 and Figure 4-8 display tabulated and graphical results, respectively, for the Tank 39 sample HGR measurements with 2000 mg/L of added glycolate. The measurements were performed in the following order: 70 °C, 85 °C, 100 °C, 105.5°C (boiling), and 35 °C (near-ambient).

The 70 °C HGR measurement showed a very similar decrease as the 70 °C for the test without glycolate. The last 80 minutes of HGR measurements at 70 °C averaged approximately 8×10^{-8} ft^3 h^{-1} gal^{-1}, indicating little to no contribution to HGR from glycolate at 70 °C for Tank 39. For the subsequent measurements, HGR at 85 °C averaged 1.9×10^{-7} ft^3 h^{-1} gal^{-1} over 1.5 hours, HGR at 100 °C averaged 8.4×10^{-7} ft^3 h^{-1} gal^{-1} over the last 2 hours, and HGR at the Tank 39 sample boiling point of 105.5 °C averaged 3.74×10^{-6} ft^3 h^{-1} gal^{-1}. Each condition above 70 °C, including the 105.5 °C condition, exhibited increasing HGR. This behavior is often seen during glycolate HGR measurements, and this trend may indicate that a reactive intermediate may build in before HGR will peak. Subsequent cooling and measurement at 35 °C resulted in an HGR below the LOQ.

In addition to the as-measured HGR from the Tank 39 test with 2000 mg/L added glycolate, Table 4-4 also contains values for the HGR adjusted to reflect the contribution exclusively due to the added glycolate.

Table 4-4. HGR measurements for Tank 39 sample with 2000 mg/L of added glycolate

T (°C)	HGR (ft^3 h^{-1} gal^{-1})		95% CI
	as measured[a]	adjusted[b]	
35	<6.4E-08	--	--
70	8E-08	--	--
85	1.9E-07	1.2E-07	± 6.1%
100	8.4E-07	7.6E-07	± 6.1%
105.5	3.74E-06	3.60E-06	± 6.1%

[a]the as-measured HGR includes both glycolate and non-glycolate related hydrogen generation
[b]the adjusted HGR subtracts non-glycolate related HGR from the as-measured HGR to yield glycolate thermolysis HGR

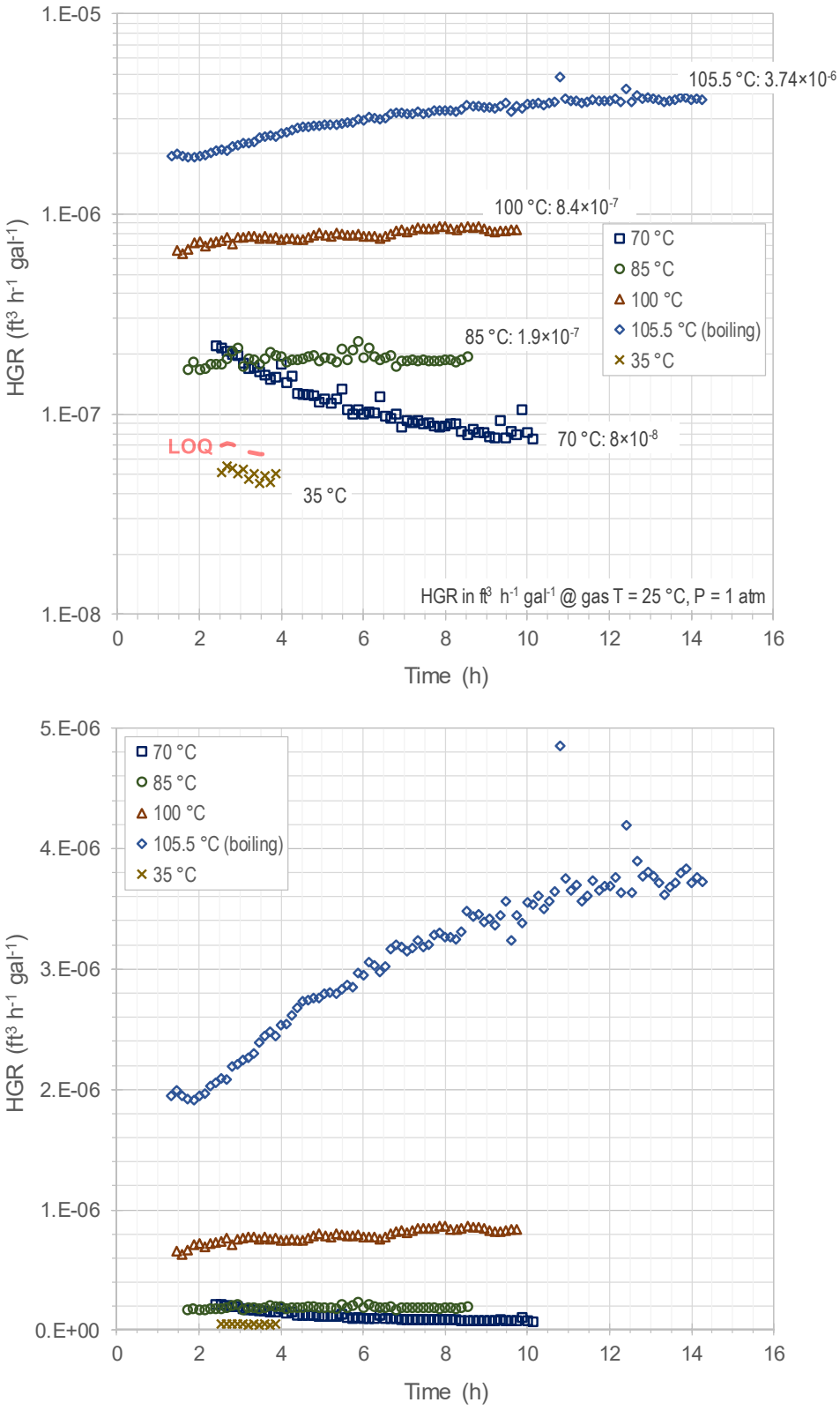

Figure 4-8. HGR measurement for Tank 39 sample with 2000 mg/L of added glycolate at a series of temperatures, logarithmic (top) and linear (bottom) scales

From Figure 4-9 and Figure 4-10, the as-measured HGR and the adjusted HGR show some degree of linearity but are not as linear as many of the past HGR tests for glycolate. The activation energies for the as-measured and adjusted HGR (153 and 178 kJ/mol, respectively) are high relative to the analogous measurements for the Tank 28 sample and other CSTF samples. Both observations can be explained by the possibility that the measurement was not held at equilibrium long enough for the lower temperature conditions to allow for the buildup of a reactive intermediate. There is a possibility that the measurements below the boiling condition are biased low, resulting in a an apparently higher activation energy.

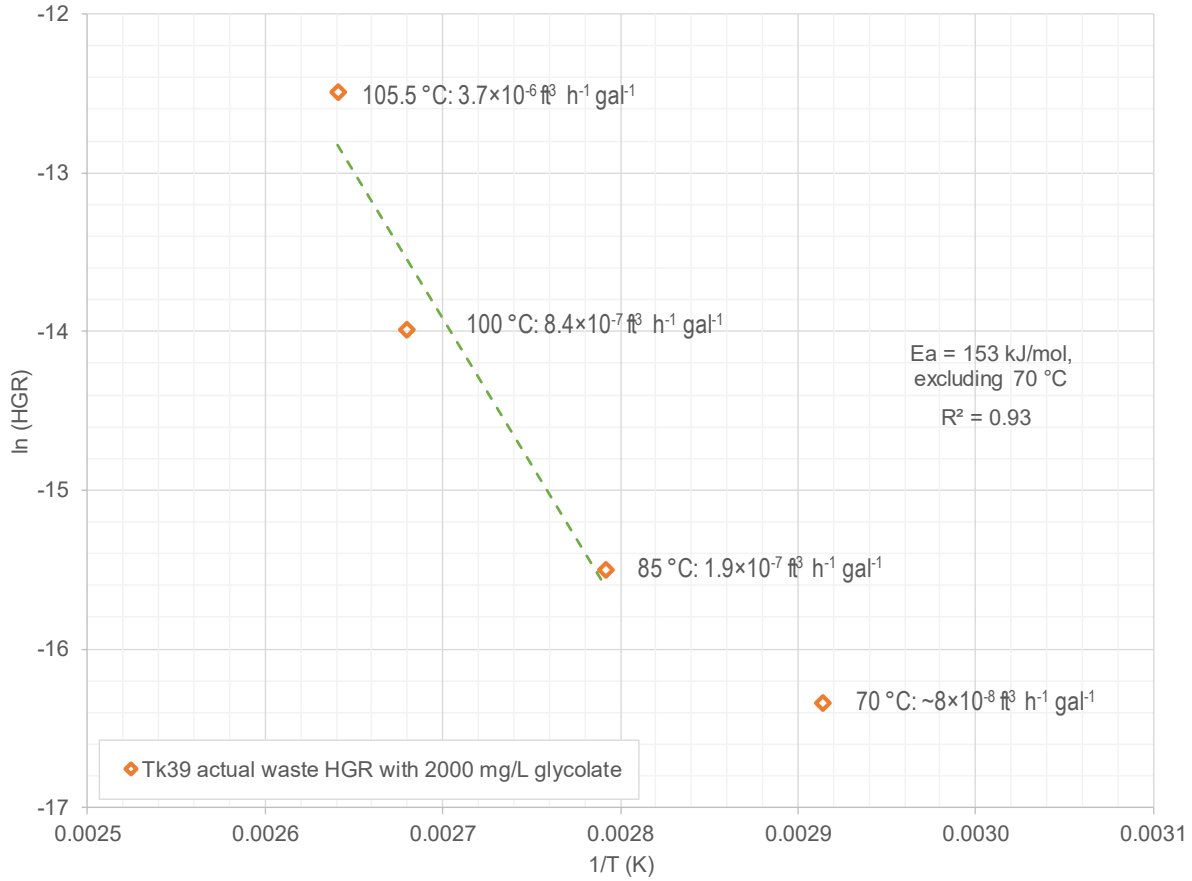

Figure 4-9. Arrhenius plot for hydrogen generation of Tank 39 sample with 2000 mg/L of added glycolate

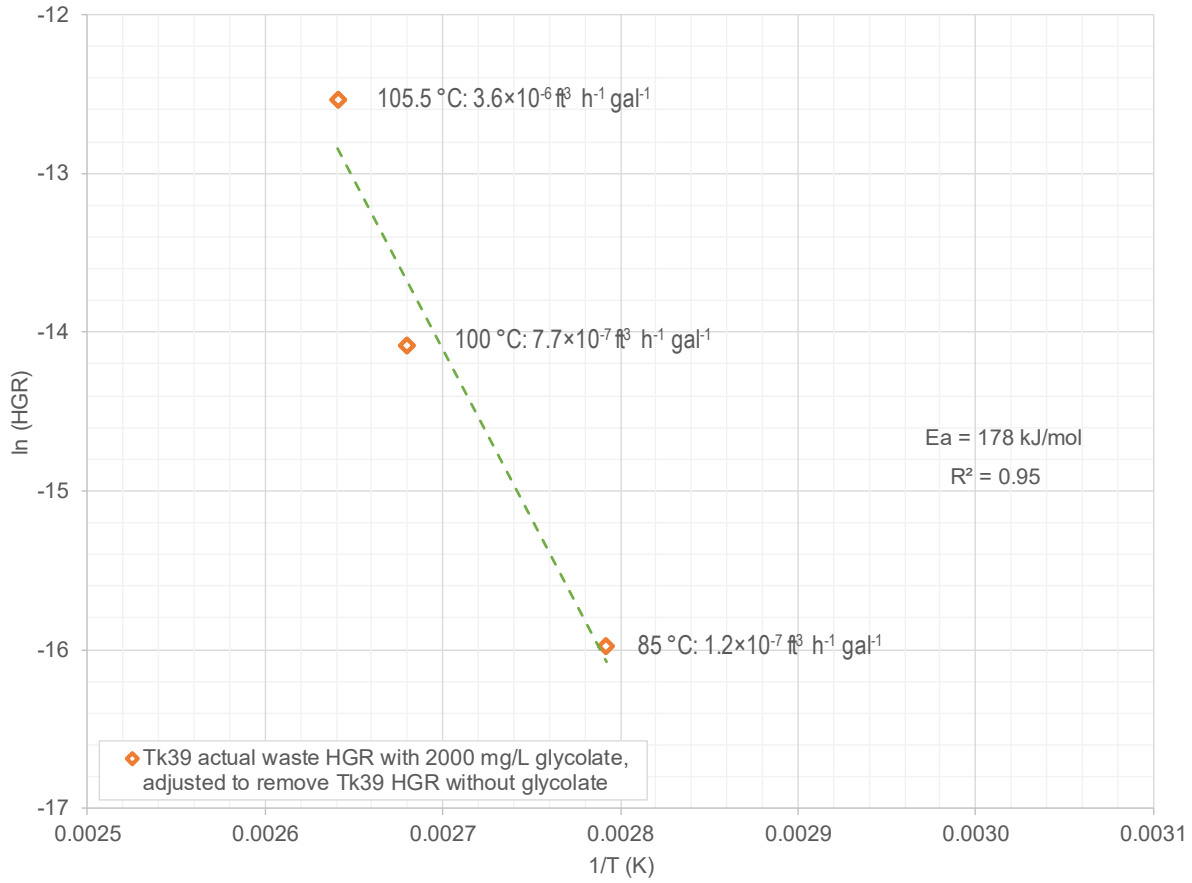

Figure 4-10. Arrhenius plot for hydrogen generation of Tank 39 sample with 2000 mg/L of added glycolate, adjusted to remove the contribution of the Tank 39 sample without glycolate

4.4.2 Other Gas Generation

Neither methane nor nitrous oxide were generated at detectable concentrations during Tank 39 sample HGR measurements with 2000 mg/L of added glycolate over the full temperature range. The 3.2 mL/min purge rate used during this testing would have allowed for the greatest chance of detecting these gasses. Carbon dioxide was measured at approximately 0.003 to 0.007 mol % and appeared to have an inverse temperature dependence. Carbon dioxide data can be seen in Appendix D.

5.0 Conclusions

The following are key results from the Tank 28 HGR testing.

- For the sample without added glycolate, the first several HGR measurements at 70, 85, and 100 °C showed little increase over the temperature range, measuring approximately 6.7×10^{-7}, 6.1×10^{-7}, and 8.1×10^{-7} $ft^3\ h^{-1}\ gal^{-1}$, respectively. Upon increasing the temperature to the Tank 28 sample boiling point, 124.8 °C, the thermolytic HGR increased to 6.27×10^{-6} $ft^3\ h^{-1}\ gal^{-1}$. A second 70 °C HGR measurement was then performed, which showed a notable decline to 1.3×10^{-7} $ft^3\ h^{-1}\ gal^{-1}$.
- Using the measurements at 100 °C, boiling at 124.8 °C, and the second measurement at 70 °C, the activation energy without added glycolate is 80 kJ/mol.
- The HGR with 500 mg/L of added glycolate at 70, 85, 100, and 124.8 °C were 1.42×10^{-6}, 3.02×10^{-6}, 1.17×10^{-5}, and 1.42×10^{-4} $ft^3\ h^{-1}\ gal^{-1}$, respectively.

- Using the measurements at 85 °C and above, the activation energy with 500 mg/L of added glycolate is 115 kJ/mol. Factoring out the thermolytic HGR from the sample material and considering only the thermolytic HGR from 500 mg/L of glycolate in the solution (at 70 °C and above) the activation energy is 108 kJ/mol.
- For the test without added glycolate, methane was generated at levels near or below the 14 ppmv (5.7×10^{-7} ft^3 h^{-1} gal^{-1}) LOQ during boiling. Methane was not detected for the test with 500 mg/L added glycolate. Carbon dioxide and nitrous oxide were also released during the testing without and with added glycolate.

The following are key results from the Tank 39 HGR testing.

- For the sample without added glycolate, the 70, 85, and 100 °C HGR measurements (7×10^{-8}, 7×10^{-8}, and 8×10^{-8} ft^3 h^{-1} gal^{-1}, respectively) all showed decreasing trends. The HGR measurement at the boiling condition of 105.3 °C was 1.4×10^{-7} ft^3 h^{-1} gal^{-1}. The activation energy was not calculated since quasi-steady state HGR values were not indicated in most experiments.
- The HGR with 2000 mg/L of added glycolate at 70, 85, 100, and 105.5 °C were 8×10^{-8}, 1.9×10^{-7}, 8.4×10^{-7}, and 3.74×10^{-6} ft^3 h^{-1} gal^{-1}, respectively.
- Using the measurements at 85 °C and above, the activation energy with 2000 mg/L of added glycolate is 153 kJ/mol. Factoring out the thermolytic HGR from the sample material and considering only the thermolytic HGR from 2000 mg/L of glycolate in the solution, the activation energy is 178 kJ/mol.
- No methane or nitrous oxide was detected during the Tank 39 sample testing without and with added glycolate. Carbon dioxide was observed during testing.

6.0 Path Forward

The HGR data for Tank 28 and 39 samples with and without added glycolate will be compared to the simulant models for glycolate and tank farm organics thermolytic HGR. The Tank 28 and 39 data can be used to assist in qualification of those models.

7.0 References

[1] Condon, W. A., “Potentially inadequate recognition of the effect of organics on hydrogen generation rates in CSTF.”, PI-2017-0003, February 28, 2017.

[2] Staub, A. V., “Potentially inadequate recognition of the effect of organics on hydrogen generation rates in Saltstone”, PI-2017-0002, February 28, 2017.

[3] Brotherton, K. M., “Potentially inadequate recognition of the effect of organics on hydrogen gas generation rates in DWPF process vessels”, PI-2017-0004, February 28, 2017.

[4] Adu-Wusu, K., “Literature Review on Impact of Glycolate on the 2H Evaporator and the Effluent Treatment Facility (ETF)”, SRNL-STI-2012-00132, Revision 0, May 2012.

[5] Ashby, E. C.; Annis, A.; Barefield, E. K.; Boatright, D.; Doctorovich, F.; Liotta, C. L.; Neumann, H. M.; Konda, A.; Yao, C. F.; Zhang, K.; and McDuffie, N. G., “Synthetic Waste Chemical Mechanism Studies”, WHC-EP-0823, Revision 0, October 1994.

[6] Bryan, S. A.; Pederson, L. R.; and King, C. M., “Thermal and Radiolytic Gas Generation in Hanford High-level Waste”, WM'00 Conference, February 27 - March 2, 2000.

[7] Crawford, C. L. and King, W. D., "Impacts of Glycolate and Formate Radiolysis and Thermolysis on Hydrogen Generation Rate Calculations for the Savannah River Site Tank Farm", SRNL-STI-2017-00303, Revision 0, August 2017.

[8] Clark, M. C., "Simulant and Radioactive Testing - Impact of Glycolate on Tank Farm", X-TTR-S-00067, Revision 2, July 9, 2018.

[9] Martino, C. J.; Woodham, W. H.; McCabe, D. J.; and Nash, C. A., "Task Technical and Quality Assurance Plan for Simulant and Radioactive Testing of the Impacts of Glycolate on Hydrogen Generation in the Savannah River Site Liquid Waste System", SRNL-RP-2017-00684, Revision 2, February 2019.

[10] Martino, C. J. and Pareizs, J. M., "Run Plan for Tank 39 Sample Thermolysis Tests Without and With Sodium Glycolate", SRNL-L3300-2019-00002, Revision 0, March 14, 2019.

[11] Martino, C. J. and Pareizs, J. M., "Run Plan for Tank 28 Sample Thermolysis Tests Without and With Sodium Glycolate", SRNL-L3300-2019-00007, Revision 0, April 2, 2019.

[12] Martino, C. J.; Newell, J. D.; Woodham, W. H.; Pareizs, J. M.; Edwards, T. B.; Lambert, D. P.; and Howe, A. M., "Investigation of Thermolytic Hydrogen Generation Rate of Tank Farm Simulated and Actual Waste", SRNL-STI-2017-00611, Revision 1, February 2019.

[13] Duignan, M. R.; Nash, C. A.; Pareizs, J. M.; Restivo, M. L.; Crawford, C. L.; and Edwards, T. B., "Hydrogen Generation Rates for Tank 50 and Saltstone Related Samples using a Sealed Reactor System", SRNL-STI-2018-00238, Revision 0, October 2018.

[14] Martino, C. J.; Newell, J. D.; Pareizs, J. M.; Duignan, M. R.; and Restivo, M. L., "Investigation of Thermolysis Hydrogen Generation Rate in Tank 38 and Tank 50 Waste Samples with Sodium Glycolate", SRNL-STI-2018-00559, Revision 0, February 2019.

[15] Martino, C. J.; Pareizs, J. M.; and Newell, J. D., "Thermolytic Hydrogen Generation Testing of Tank 22 Material", SRNL-STI-2018-00385, Revision 0, November 2018.

[16] Woodham, W. H., "Run Plan for Testing to Screen and Assess the Hydrogen Generation Rates Evolved from the Thermolysis of Glycolate and Other Prominent Tank Farm Organics", SRNL-L3300-2018-00004, Revision 0, January 29, 2018.

[17] Woodham, W. H., "Run Plan for Testing to Evaluate Importance of Major Salt Species on Thermolytic Production of Hydrogen from Glycolate", SRNL-L3300-2018-00011, Revision 1, September 26, 2018.

[18] Woodham, W. H., "Run Plan for Testing to Evaluate Influence of Major Salt Species on Thermolytic Production of Hydrogen from Prominent Tank Farm Organics and Glycolate", SRNL-L3300-2018-00056, Revision 0, October 17, 2018.

[19] Woodham, W. H. and Edwards, T. B., "Run Plan for Testing to Improve Interim Models for Thermolytic Production of Hydrogen from Glycolate and Other Prominent Tank Farm Organics", SRNL-L3300-2019-00003, Revision 0, February 14, 2019.

[20] Chen, G. and Sudduth, C. B., "Waste Tank Selection for Testing the Impact of Glycolate and Existing Tank Farm Organics on Thermolytic Hydrogen Generation Rate", X-ESR-G-00066, Revision 0, April 1, 2019.

[21] Martino, C. J.; McCabe, D. J.; Edwards, T. B.; and Nichols, R. L., "Analysis of Tank 28F Saltcake Core Samples FTF-456 – 467", WSRC-STI-2006-00151, Revision 0, February 28, 2007.

[22] Hu, T. A., "Empirical Rate Equation Model and Rate Calculations of Hydrogen Generation for Hanford Tank Waste", HNF-3851, Revision 1, September 2004.

[23] Martino, C. J. and Edwards, T. B., "Run Plan for Tank 22 Sample Thermolysis Tests", SRNL-L3300-2018-00001, Revision 0, March 28, 2018.

[24] Newell, J. D.; Pareizs, J. M.; Martino, C. J.; Reboul, S. H.; Coleman, C. J.; Edwards, T. B.; and Johnson, F. C., "Actual Waste Demonstration of the Nitric-Glycolic Flowsheet for Sludge Batch 9 Qualification", SRNL-STI-2016-00327, Revision 1, March 9, 2017.

[25] Pareizs, J. M.; Newell, J. D.; Martino, C. J.; Crawford, C. L.; and Johnson, F. C., "Sludge Washing and Demonstration of the DWPF Nitric/Formic Flowsheet in the SRNL Shielded Cells for Sludge Batch 9 Qualification", SRNL-STI-2016-00355, Revision 0, October 2016.

[26] Stone, M. E.; Adamson, D. J.; Pak, D. J.; and Pareizs, J. M., "Hydrogen Generation Rate Measurement Apparatus: Final Design Package", SRNL-RP-2014-00866, Revision 0, September 2014.

[27] Stone, M. E.; Newell, J. D.; Smith, T. E.; and Pareizs, J. M., "WTP Waste Feed Qualification: Hydrogen Generation Rate Measurement Apparatus Testing Report", SRNL-STI-2016-00247, Revision 0, June 2016.

[28] Reboul, S. H.; Newell, J. D.; Pareizs, J. M.; and Coleman, C. J., "Low Temperature Aluminum Dissolution (LTAD) Real Waste Testing of the November 2017 Tank 51 Slurry Sample", SRNL-STI-2018-00179, Revision 0, June 2018.

[29] Metrodata GmbH, "GUM Workbench: User Manual for Version 1.3, 2.3, and 2.4", 2009.

[30] "SAS Institute Inc., JMP™ Pro, Ver. 11.2.1", Cary, NC, 2014.

[31] "Definition and Procedure for the Determination of the Method Detection Limit-Revision 2", 40 CFR, Part 136, Appendix B, 2017.

[32] Taylor, J. K., *Quality Assurance of Chemical Measurements*. Lewis Publishers, Inc.: Chelsea, MI, 1987.

[33] "Technical Reviews", Manual E7, Procedure 2.60, Revision 17, August 25, 2016.

[34] "Savannah River National Laboratory Technical Report Design Check Guidelines", WSRC-IM-2002-00011, Revision 2, August 2004.

[35] Newell, J. D., "1L SRAT ACTL LAB132 DACS", B-SWCD-A-00741, Revision 0, 2017.

[36] Edwards, T. B., "GUM Workbench Version 2.4.1.411", B-SWCD-W-00022, Revision 0, 2014.

[37] Edwards, T. B., "JMP Pro Version 11.2.1", B-SWCD-W-00023, Revision 0, 2014.

[38] Baker, R. A.; Edwards, T. B.; Elizondo, A. D.; Harris, S. P.; Shine, E. P.; and Watson, H. L., "Verification & Validation for Commercial Statistical Packages Utilized by SRNL Statisticians", B-VVR-A-00002, Revision 3, December 2014.

Appendix A. Test Process

Test 1: The testing process for Tank 28 sample supernate with no added glycolate is as follows:

1. Load the system with approximately 1.06 L (1610 g) of Tank 28 sample supernate
2. Agitate sample and initiate purge gas flow
3. Heat to 70 °C
4. Adjust purge gas flow to the measurement purge rate
5. Allow the system to equilibrate and measure the HGR at 70 °C
6. Increase purge and heat to 85 °C
7. Adjust purge gas flow to the measurement purge rate
8. Allow the system to equilibrate and measure the HGR at 85 °C
9. Increase purge and heat to 100 °C
10. Adjust purge gas flow to the measurement purge rate
11. Allow the system to equilibrate and measure the HGR at 100 °C
12. Increase purge and heat to the atmospheric pressure boiling point of the mixture
13. Adjust purge gas flow to the measurement purge rate
14. Allow the system to equilibrate and measure the HGR at boiling
15. Increase purge and allow the system to cool to 70 °C, control temperature (heat) to 70 °C
16. Adjust purge gas flow to the measurement purge rate
17. Allow the system to equilibrate and measure the HGR at 70 °C
18. Increase purge and allow the system to cool to 40 °C, control temperature (heat) to 40 °C
19. Adjust purge gas flow to the measurement purge rate
20. Allow the system to equilibrate and measure the HGR at 40 °C
21. Shutdown the system and unload the Tank 28 material
22. Subsample the Tank 28 material for post-HGR chemical analysis
23. Clean and reassemble the system

Test 2: The testing process for Tank 39 sample supernate with no added glycolate is as follows:

1. Load the system with approximately 1.06 L (1360 g) of Tank 39 sample supernate
2. Agitate sample and initiate purge gas flow
3. Heat to 70 °C
4. Adjust purge gas flow to the measurement purge rate
5. Allow the system to equilibrate and measure the HGR at 70 °C
6. Increase purge and heat to 85 °C
7. Adjust purge gas flow to the measurement purge rate
8. Allow the system to equilibrate and measure the HGR at 85 °C
9. Increase purge and heat to 100 °C
10. Adjust purge gas flow to the measurement purge rate
11. Allow the system to equilibrate and measure the HGR at 100 °C
12. Increase purge and heat to the atmospheric pressure boiling point of the mixture
13. Adjust purge gas flow to the measurement purge rate
14. Allow the system to equilibrate and measure the HGR at boiling
15. Increase purge and allow the system to cool to 35 °C, control temperature (heat) to 35 °C
16. Adjust purge gas flow to the measurement purge rate
17. Allow the system to equilibrate and measure the HGR at 35 °C
18. Shutdown the system and unload the Tank 39 material
19. Subsample the Tank 39 material for post-HGR chemical analysis
20. Clean and reassemble the system

Test 3: The testing process for Tank 39 sample supernate with 2000 mg/L glycolate added as sodium glycolate is as follows:

1. Load the system with approximately 1.06 L of Tank 39 sample supernate and 2.7949 g of 99.1 wt% sodium glycolate (corresponding to 2.24 g or 2.00 g/L of glycolate)
2. Agitate sample and initiate purge at an increased rate
3. Heat to 70 °C
4. Collect an approximately 20-gram sample from the system. At this point, the sample volume remaining in the system will be approximately 1 L (1360 g).
5. Reestablish agitation and purge gas flow, if necessary, and heat to 70 °C
6. Adjust purge gas flow to the measurement purge rate
7. Allow the system to equilibrate and measure the HGR at 70 °C
8. Increase purge and heat to 85 °C
9. Adjust purge gas flow to the measurement purge rate
10. Allow the system to equilibrate and measure the HGR at 85 °C
11. Increase purge and heat to 100 °C
12. Adjust purge gas flow to the measurement purge rate
13. Allow the system to equilibrate and measure the HGR at 100 °C
14. Increase purge and heat to the atmospheric pressure boiling point of the mixture
15. Adjust purge gas flow to the measurement purge rate
16. Allow the system to equilibrate and measure the HGR at boiling
17. Increase purge and allow the system to cool to 35 °C, control temperature (heat) to 35 °C
18. Adjust purge gas flow to the measurement purge rate
19. Allow the system to equilibrate and measure the HGR at 35 °C
20. Shutdown the system and unload the Tank 39 material
21. Subsample the Tank 39 material for post-HGR chemical analysis
22. Clean and reassemble the system

Test 4: The testing process for Tank 28 sample supernate with 500 mg/L glycolate added as sodium glycolate is as follows:

1. Load the system with approximately 1.06 L of Tank 28 sample supernate and 0.6989 g of 99.1 wt% sodium glycolate (corresponding to 560 mg or 500 mg/L of glycolate)
2. Agitate sample, initiate purge gas flow at an increased rate
3. Heat to 70 °C
4. Collect an approximately 20-gram sample from the system. At this point, the sample volume remaining in the system will be approximately 1.1 L (1610 g).
5. Reestablish agitation and purge gas flow, if necessary, and heat to 70 °C
6. Adjust purge gas flow to the measurement purge rate
7. Allow the system to equilibrate and measure the HGR at 70 °C
8. Increase purge and heat to 85 °C
9. Adjust purge gas flow to the measurement purge rate
10. Allow the system to equilibrate and measure the HGR at 85 °C
11. Increase purge and heat to 100 °C
12. Adjust purge gas flow to the measurement purge rate
13. Allow the system to equilibrate and measure the HGR at 100 °C
14. Increase purge and heat to the atmospheric pressure boiling point of the mixture
15. Adjust purge gas flow to the measurement purge rate
16. Allow the system to equilibrate and measure the HGR at boiling
17. Increase purge and allow the system to cool to 35 °C, control temperature (heat) to 35 °C
18. Adjust purge gas flow to the measurement purge rate
19. Allow the system to equilibrate and measure the HGR at 35 °C
20. Shutdown the system and unload the Tank 28 material
21. Subsample the Tank 28 material for post-HGR chemical analysis
22. Clean and reassemble the system

Appendix B. Additional Analytical Results

Table B-1. Below detection limit values for Tank 28 sample analysis

analyte	method	units	Tank 28 without glycolate		Tank 28 with 500 mg/L glycolate
			feed	post HGR	post HGR
F^-	IC	M	<7.6E-03	<1.9E-01	<9.6E-02
Br^-	IC	M	<9.0E-03	<4.5E-02	<2.3E-02
Ag	ICP-ES	mg/L	<7.4E+00	<7.2E+00	<7.2E+00
Ba	ICP-ES	mg/L	<7.4E+00	<7.2E+00	<7.2E+00
Be	ICP-ES	mg/L	<7.4E+00	<7.2E+00	<7.2E+00
Cd	ICP-ES	mg/L	<7.4E+00	<7.2E+00	<7.2E+00
Ce	ICP-ES	mg/L	<7.4E+00	<7.2E+00	<7.2E+00
Co	ICP-ES	mg/L	<7.4E+00	<7.2E+00	<7.2E+00
Cu	ICP-ES	mg/L	<7.4E+00	<7.2E+00	<7.2E+00
Gd	ICP-ES	mg/L	<7.4E+00	<7.2E+00	<7.2E+00
La	ICP-ES	mg/L	<7.4E+00	<7.2E+00	<7.2E+00
Li	ICP-ES	mg/L	<7.4E+00	<7.2E+00	<7.2E+00
Mg	ICP-ES	mg/L	<7.4E+00	<7.2E+00	<7.2E+00
Mn	ICP-ES	mg/L	<7.4E+00	<7.2E+00	<7.2E+00
Ni	ICP-ES	mg/L	<7.4E+00	<1.3E+01	<2.3E+01
Pb	ICP-ES	mg/L	<1.1E+02	<2.3E+01	<1.6E+01
Sb	ICP-ES	mg/L	<7.4E+00	<7.2E+00	<7.2E+00
Sn	ICP-ES	mg/L	<5.0E+01	<8.3E+00	<1.1E+01
Sr	ICP-ES	mg/L	<7.4E+00	<7.2E+00	<7.2E+00
Th	ICP-ES	mg/L	<7.4E+00	<7.2E+00	<7.2E+00
Ti	ICP-ES	mg/L	<7.4E+00	<7.2E+00	<7.2E+00
U	ICP-ES	mg/L	<2.3E+01	<4.8E+01	<2.0E+01
V	ICP-ES	mg/L	<7.4E+00	<7.2E+00	<7.2E+00
Zr	ICP-ES	mg/L	<7.4E+00	<7.2E+00	<7.2E+00

Table B-2. Below detection limit values for Tank 39 sample analysis

analyte	method	units	Tank 39 without glycolate		Tank 39 with 2 g/L glycolate
			feed	post HGR	post HGR
PO_4^{3-}	IC	M	<7.0E-04	<1.3E-02	<6.8E-03
Cl^-	IC	M	<1.9E-03	<3.5E-02	<1.8E-02
F^-	IC	M	<3.5E-03	<6.4E-02	<3.4E-02
Br^-	IC	M	<4.2E-03	<1.5E-02	<8.1E-03
Ag	ICP-ES	mg/L	<6.1E+00	<2.4E+00	<2.5E+00
Ba	ICP-ES	mg/L	<6.1E+00	<2.4E+00	<2.5E+00
Be	ICP-ES	mg/L	<6.1E+00	<2.4E+00	<2.5E+00
Cd	ICP-ES	mg/L	<6.1E+00	<2.4E+00	<2.5E+00
Ce	ICP-ES	mg/L	<6.1E+00	<2.4E+00	<2.5E+00
Co	ICP-ES	mg/L	<6.1E+00	<2.4E+00	<2.5E+00
Cu	ICP-ES	mg/L	<6.1E+00	<2.4E+00	<2.5E+00
Gd	ICP-ES	mg/L	<6.1E+00	<2.4E+00	<2.5E+00
La	ICP-ES	mg/L	<6.1E+00	<2.4E+00	<2.5E+00
Li	ICP-ES	mg/L	<6.1E+00	<2.4E+00	<2.5E+00
Mg	ICP-ES	mg/L	<6.1E+00	<2.4E+00	<2.5E+00
Ni	ICP-ES	mg/L	<6.1E+00	<4.4E+00	<8.2E+00
Pb	ICP-ES	mg/L	<9.5E+01	<2.4E+00	<5.5E+00
Sb	ICP-ES	mg/L	<6.1E+00	<2.4E+00	<2.5E+00
Sn	ICP-ES	mg/L	<4.1E+01	<2.8E+00	<3.7E+00
Sr	ICP-ES	mg/L	<6.1E+00	<2.4E+00	<2.5E+00
Th	ICP-ES	mg/L	<6.1E+00	<2.4E+00	<2.5E+00
Ti	ICP-ES	mg/L	<6.1E+00	<2.4E+00	<2.5E+00
U	ICP-ES	mg/L	<1.9E+01	<1.6E+01	<7.0E+00
V	ICP-ES	mg/L	<6.1E+00	<2.4E+00	<2.5E+00
Zn	ICP-ES	mg/L	<6.1E+00	<2.4E+00	<2.6E+00
Zr	ICP-ES	mg/L	<6.1E+00	<2.4E+00	<2.5E+00

Appendix C. HGR Test Plots

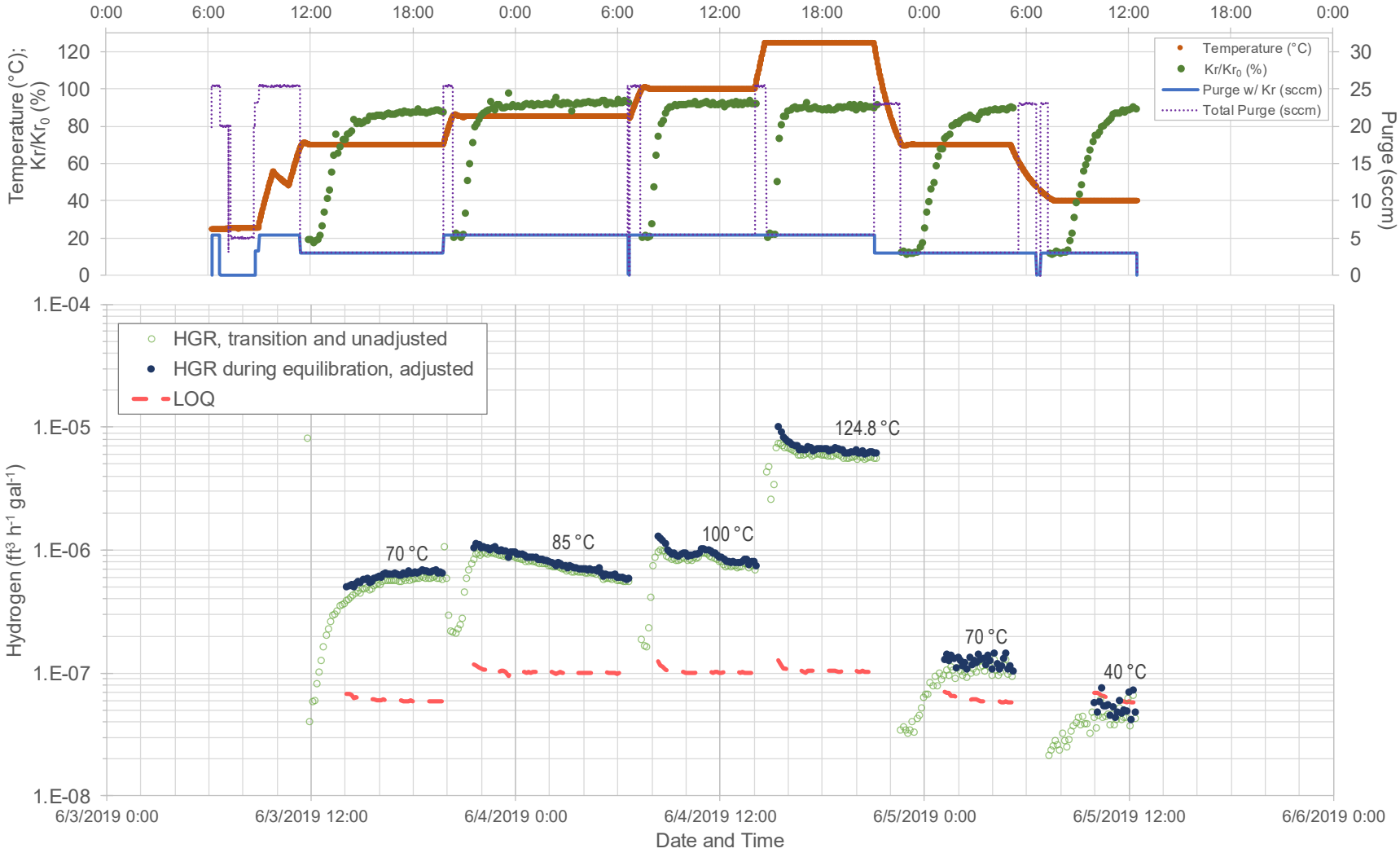

Figure C-1. Test profile for Tank 28 HGR test without added glycolate

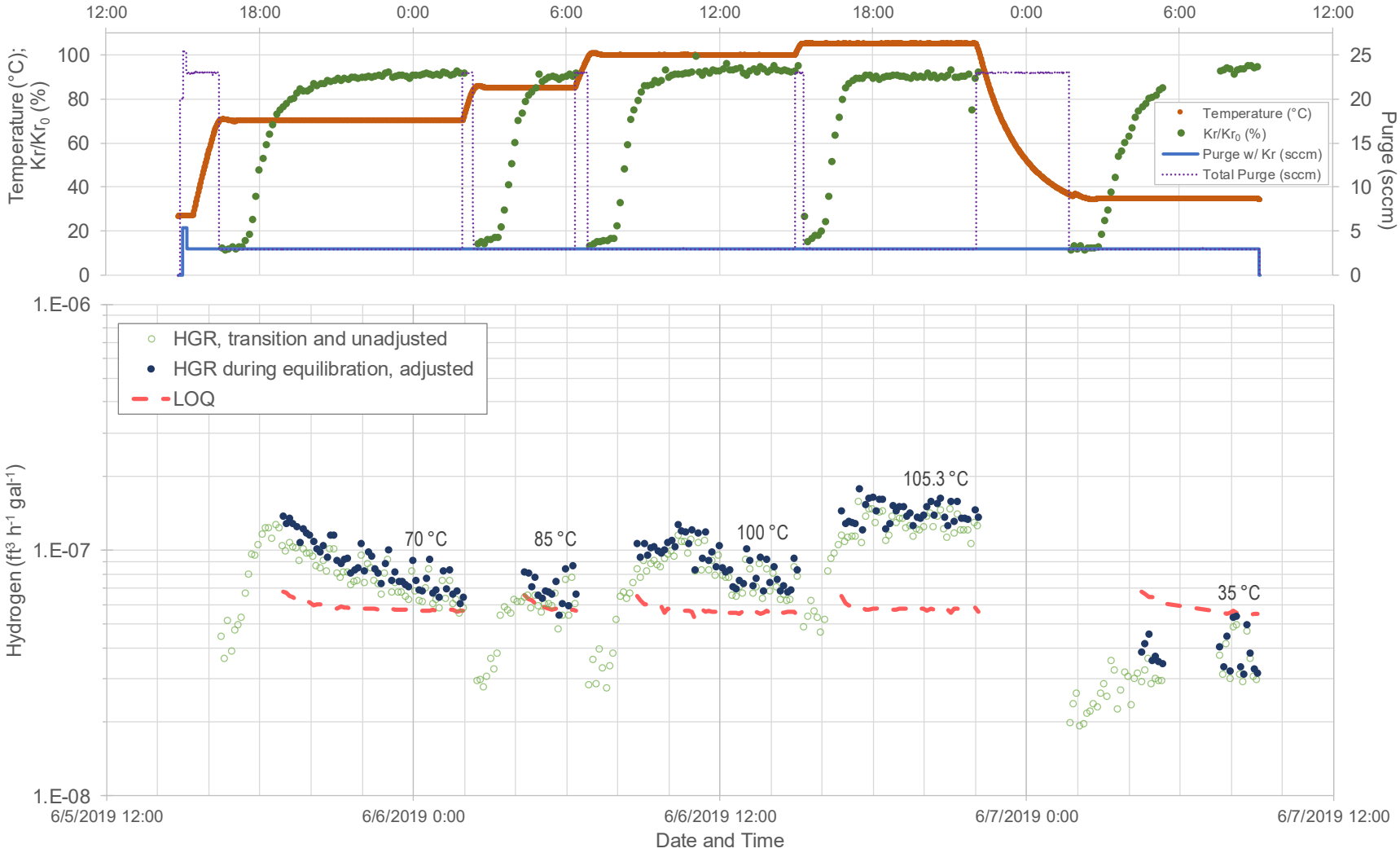

Figure C-2. Test profile for Tank 39 HGR test without added glycolate

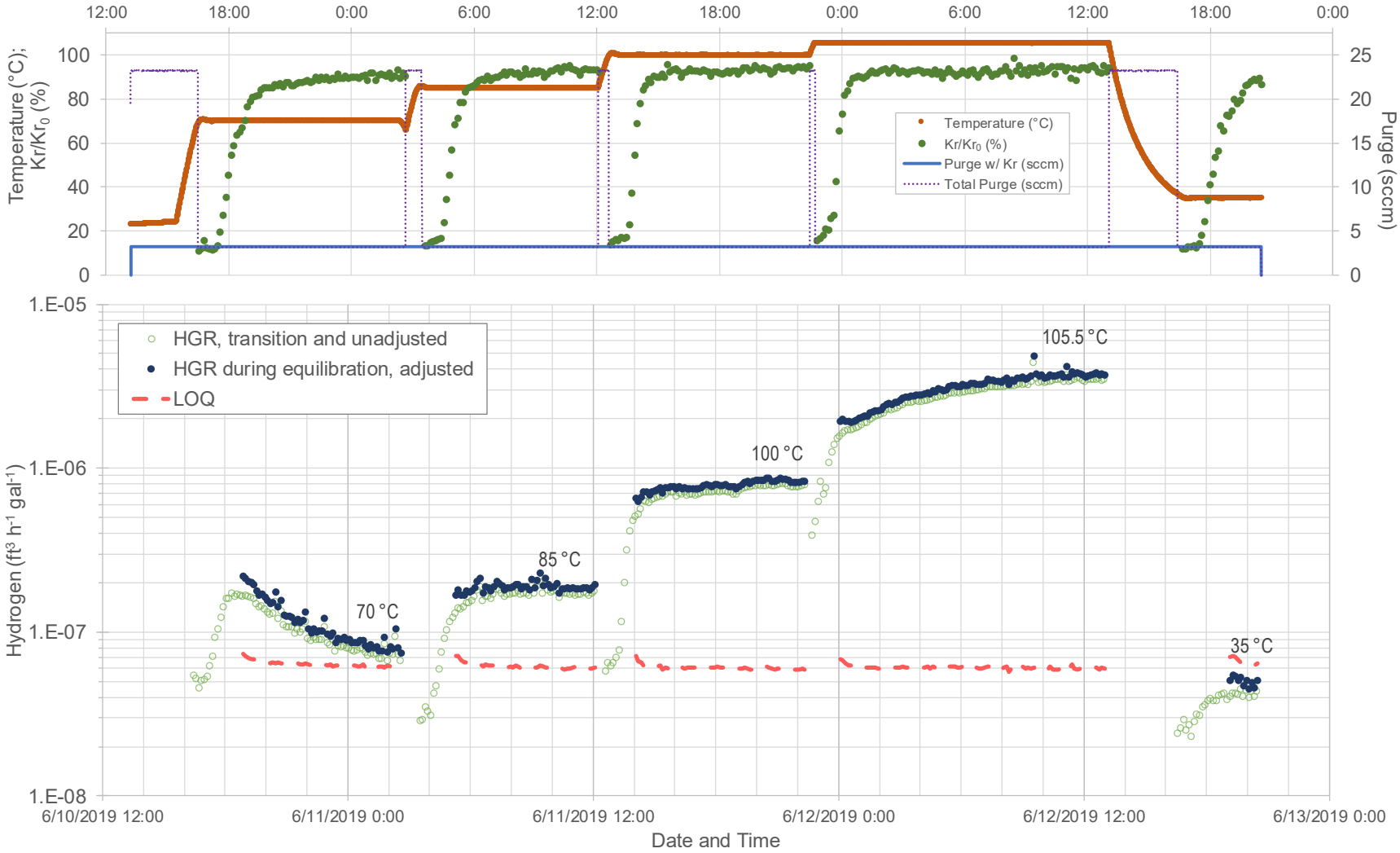

Figure C-3. Test profile for Tank 39 HGR test with added glycolate

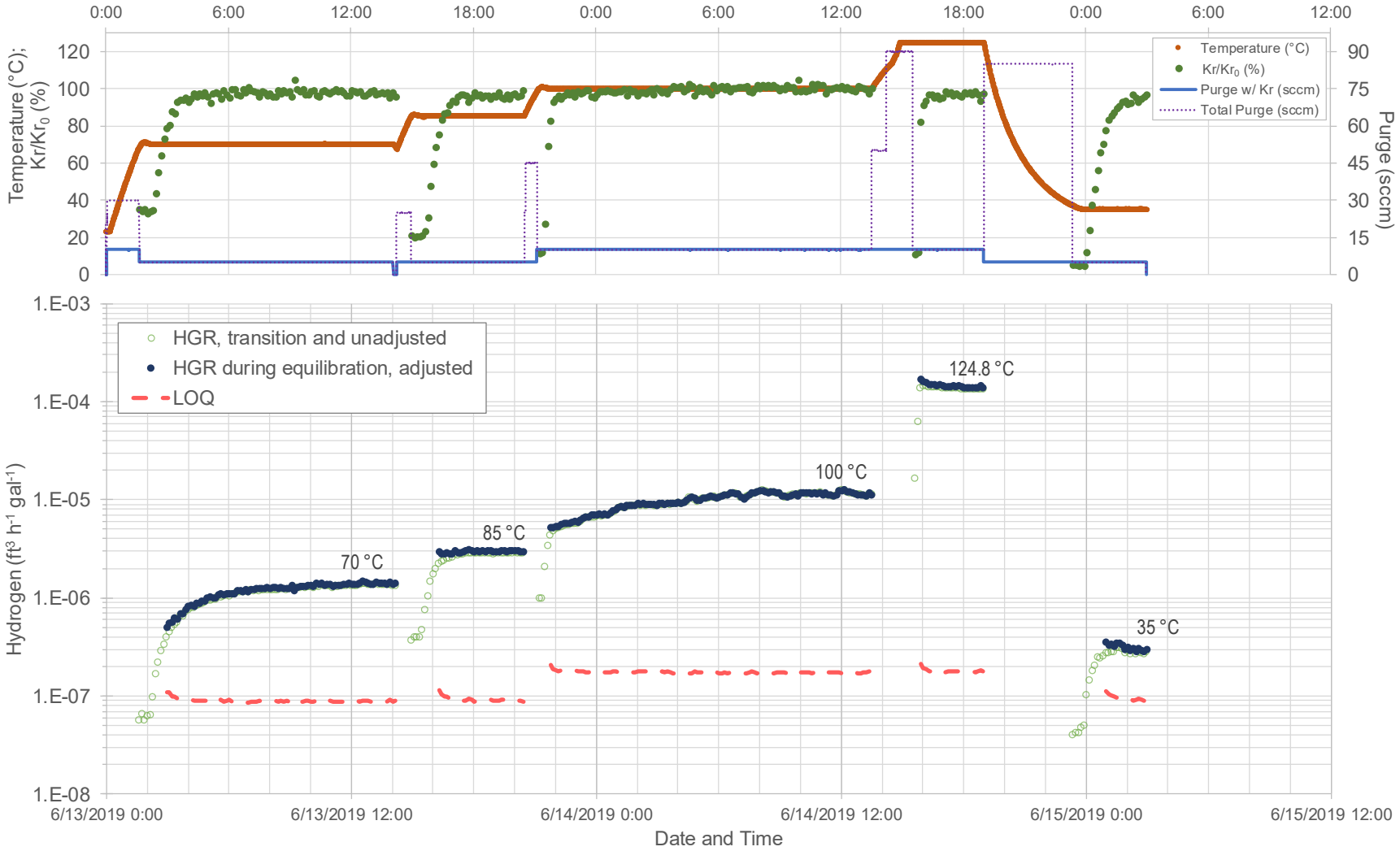

Figure C-4. Test profile for Tank 28 HGR test with added glycolate

Appendix D. Other Gas Measurement Plots

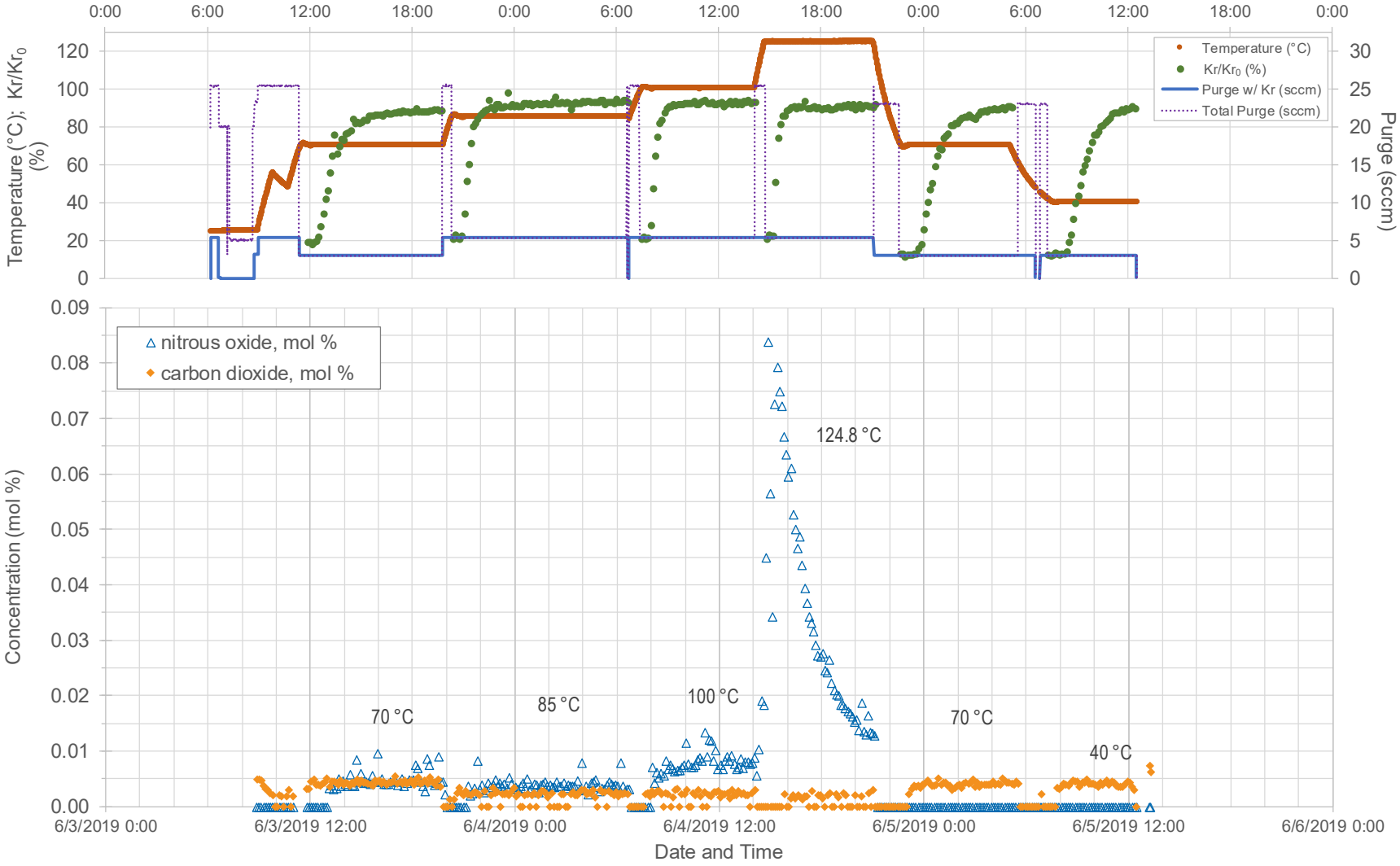

Figure D-1. Nitrous oxide and carbon dioxide vapor concentration profile for Tank 28 HGR test without added glycolate

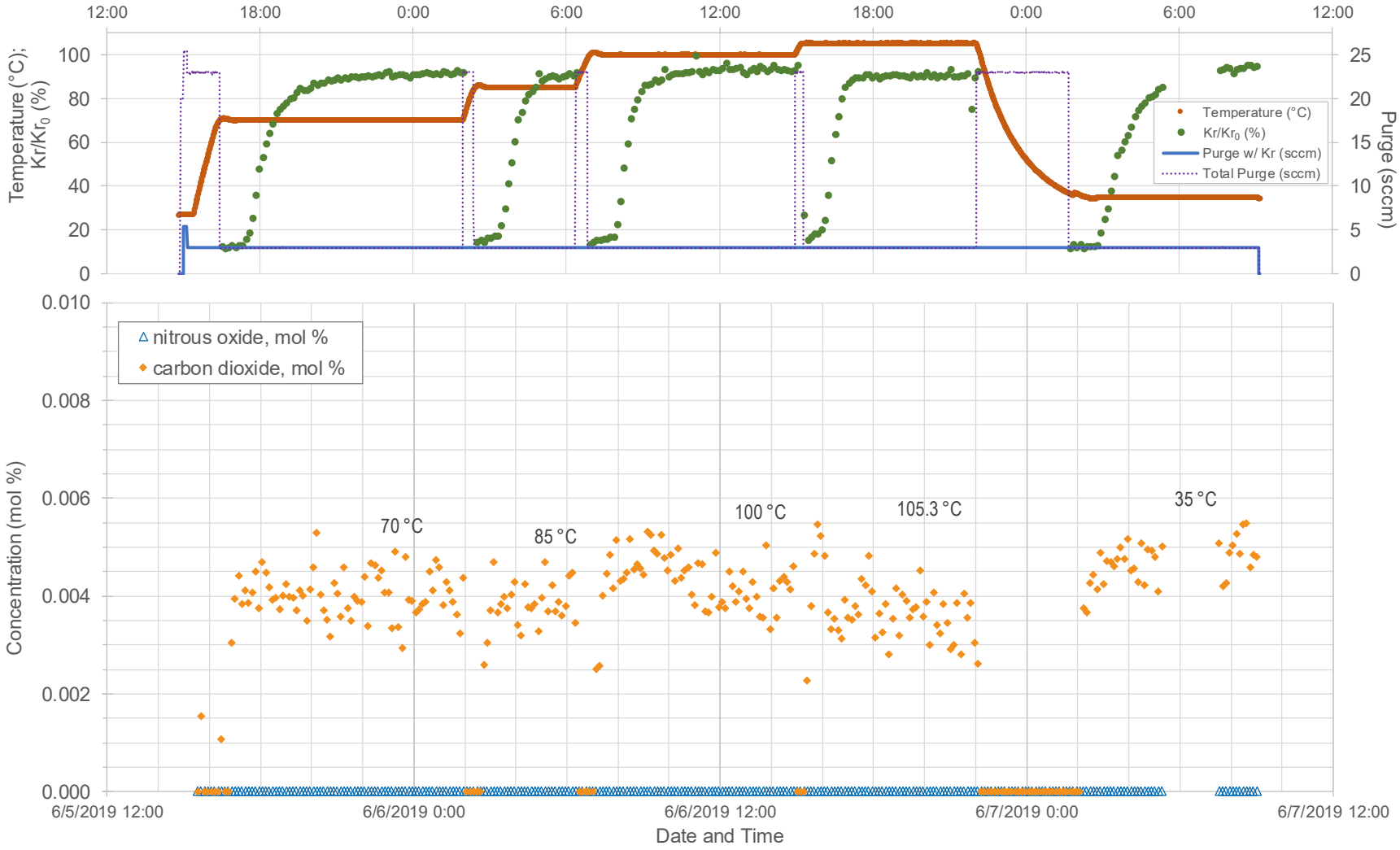

Figure D-2. Nitrous oxide and carbon dioxide vapor concentration profile for Tank 39 HGR test without added glycolate

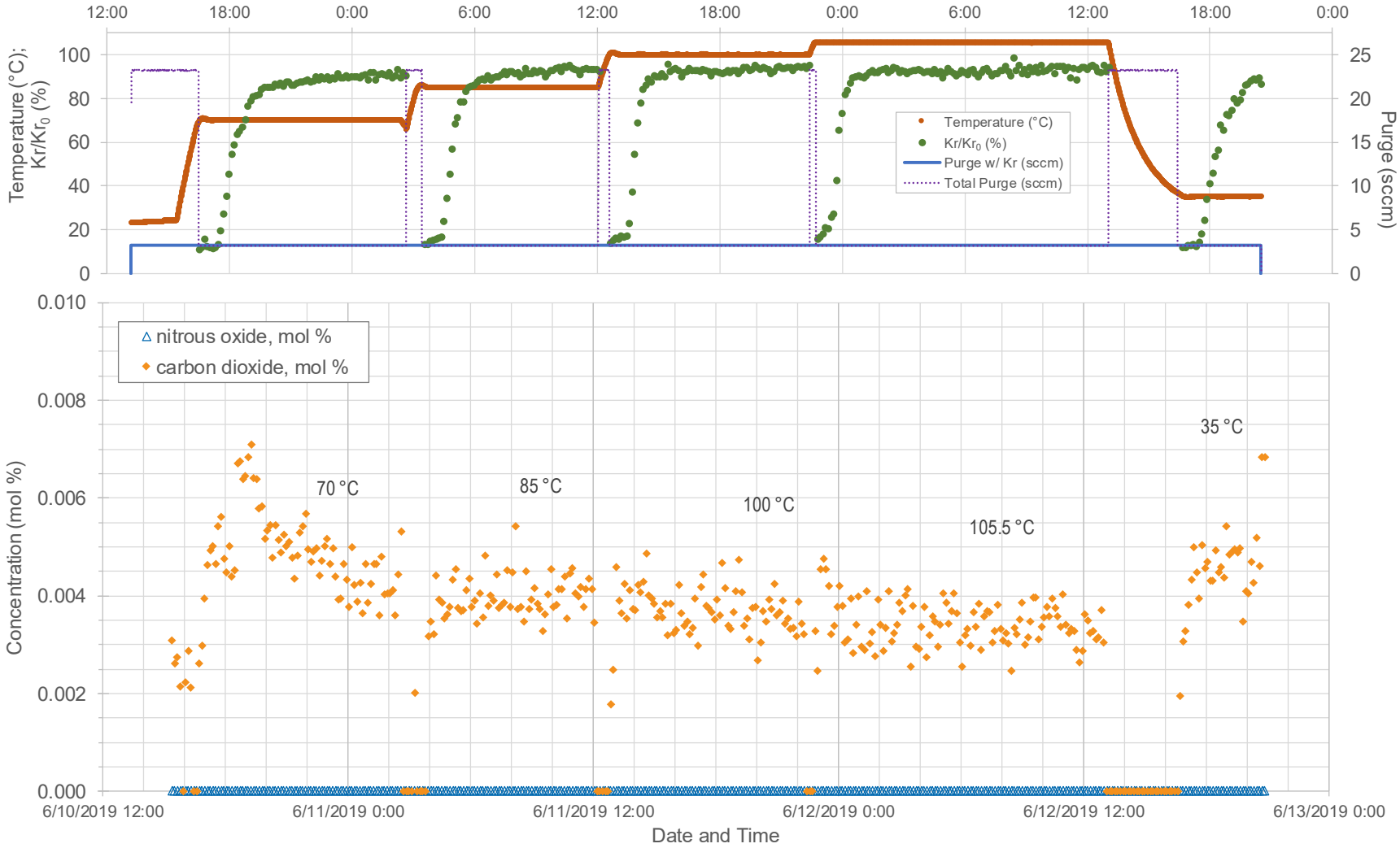

Table D-1. Nitrous oxide and carbon dioxide vapor concentration profile for Tank 39 HGR test with 2000 mg/L of added glycolate

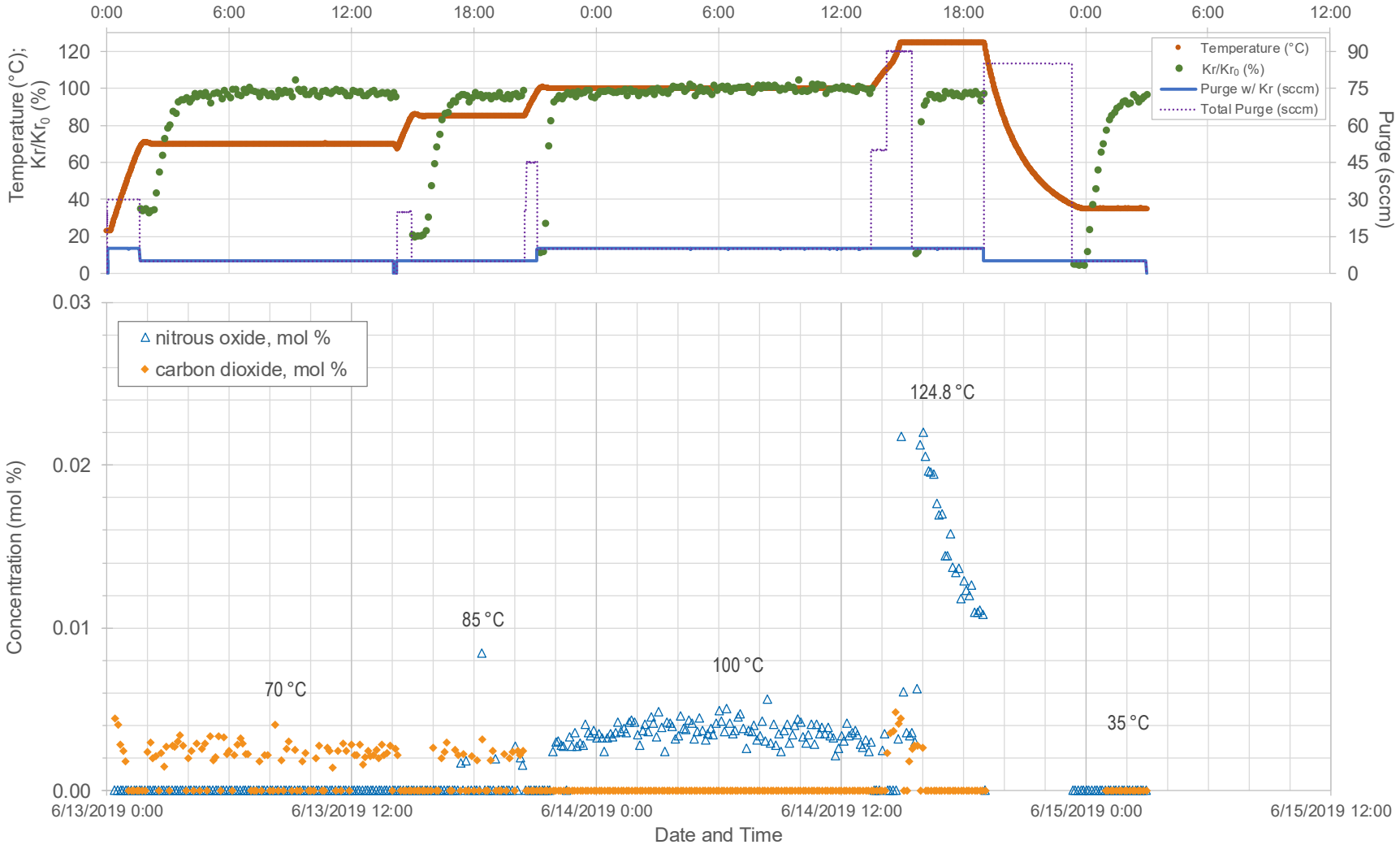

Figure D-3. Nitrous oxide and carbon dioxide vapor concentration profile for Tank 28 HGR test with 500 mg/L of added glycolate

Appendix E. Variation in Calibration Gas Area Measurements

Five sets of calibration data were collected over the course of the Tank 28 and Tank 39 sample HGR tests. From each set of calibration gas runs, the last 10 observations were considered for use in calibration. The peak area data for the hydrogen and krypton calibration are presented in Exhibit E-1 and Exhibit E-2, respectively.

The five data sets taken over the two weeks of testing were as follows:

- Set 1 – at the start of week 1, prior to the Tank 28 test without glycolate.
- Set 2 – in the middle of week 1, between the Tank 28 test without glycolate and the Tank 39 test without glycolate.
- Set 3 – at the end of week 1, near the end of the Tank 39 test without glycolate.
- Set 4 – at the start of week 2, prior to the Tank 39 test with 2000 mg/L glycolate.
- Set 5 – at the end of week 2, near the end of the Tank 28 test with 500 mg/L glycolate.

Exhibit E-1. Hydrogen Calibration Data

Variability Chart for H2 Area

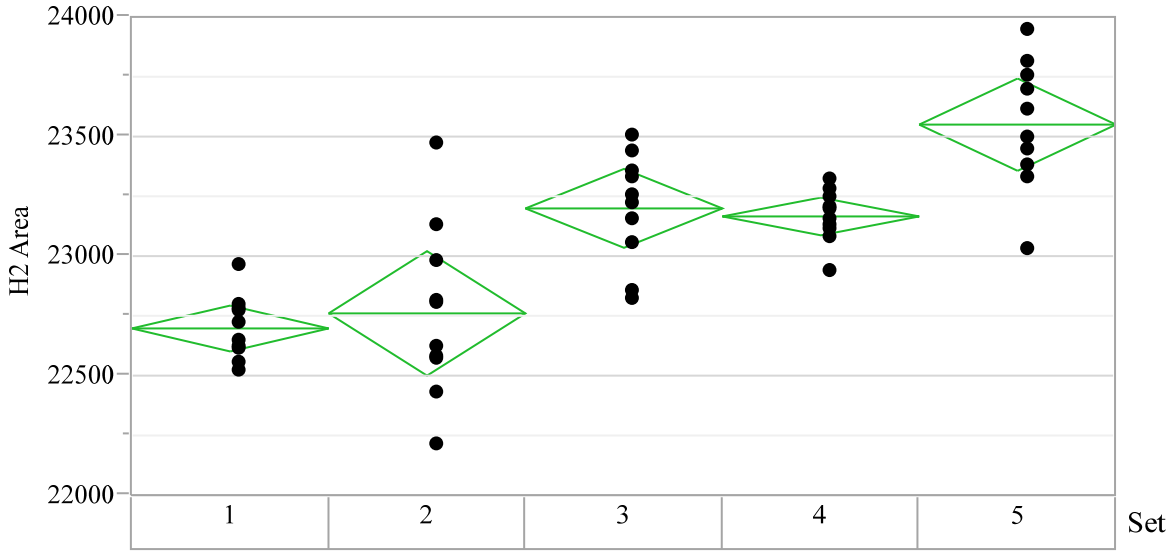

Variability Summary for H2 Area

	Mean	Std Dev	Std Err Mean	Lower 95%	Upper 95%	Minimum	Maximum	Observations
H2 Area	23078.68	391.3696	55.34802	22967.45	23189.91	22217	23946	50
Set[1]	22701.3	134.0158	42.37952	22605.43	22797.17	22523	22967	10
Set[2]	22764.5	364.1023	115.1393	22504.04	23024.96	22217	23473	10
Set[3]	23203.6	230.3708	72.84965	23038.8	23368.4	22829	23512	10
Set[4]	23170.2	110.381	34.90552	23091.24	23249.16	22940	23323	10
Set[5]	23553.8	269.7368	85.29827	23360.84	23746.76	23030	23946	10

Exhibit E-2. Krypton Calibration Data

Variability Chart for Kr Area

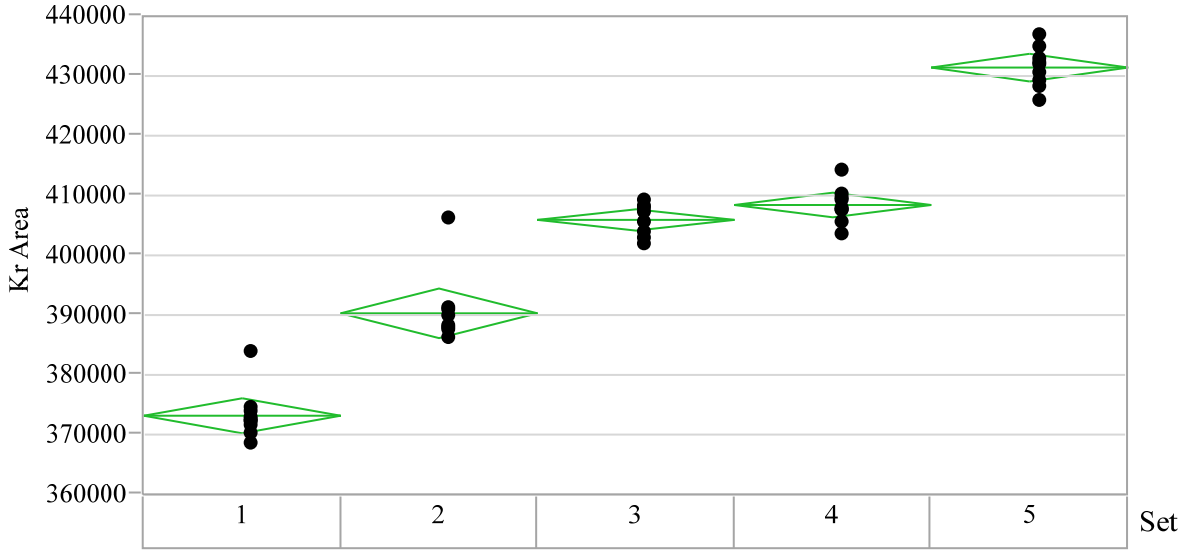

Variability Summary for Kr Area

	Mean	Std Dev	Std Err Mean	Lower 95%	Upper 95%	Minimum	Maximum	Observations
Kr Area	402009.5	19988.91	2826.858	396328.7	407690.3	368682	437097	50
Set[1]	373328.3	4109.839	1299.645	370388.3	376268.3	368682	384011	10
Set[2]	390465.3	5814.819	1838.807	386305.6	394625	386119	406194	10
Set[3]	406094.2	2492.596	788.228	404311.1	407877.3	401985	409323	10
Set[4]	408589.6	2879.65	910.6254	406529.6	410649.6	403599	414306	10
Set[5]	431570	3240.982	1024.889	429251.5	433888.5	425837	437097	10

From Exhibit E-1 and Exhibit E-2, both hydrogen and krypton calibration gas area measurements are seen to generally increase over the course of the two weeks of testing. Sets 3 and 4, near the midpoint time of the testing, have calibration gas areas that are nearest to the mean of the calibration gas area. The initial set of calibration data (Set 1) is approximately 2% and 7% below the mean areas for hydrogen and krypton, respectively. Conversely, the final set of calibration data (Set 5) is approximately 2% and 7% above the mean areas for hydrogen and krypton, respectively.

Providing thermolytic HGR measurements for potential use in safety basis calculations is amongst the goals of this testing. For this reason, calibration anomalies that impact HGR measurements are included as a potential high bias in the measurements to maintain conservatism. Examining Equation 1 in the body of this report, the calculation of HGR from GC measurements has the relationship of HGR as inversely proportional to the hydrogen calibration area and directly proportional to the krypton calibration area. Thus, to maintain conservatism in HGR, the lowest applicable hydrogen calibration areas and highest applicable krypton calibration areas were used. The HGR calculations for the first week of testing (Tank 28 and 39 without glycolate) used Set 1 for hydrogen and Set 3 for krypton. The HGR calculations for the second week of testing (Tank 39 and Tank 28 with added glycolate) used Set 4 for hydrogen and Set 5 for krypton. Overall, this approach resulted in an approximately 0% to 10% high bias in the reported HGR measurements.

Distribution:

timothy.brown@srnl.doe.gov
alex.cozzi@srnl.doe.gov
david.crowley@srnl.doe.gov
c.diprete@srnl.doe.gov
a.fellinger@srnl.doe.gov
samuel.fink@srnl.doe.gov
nancy.halverson@srnl.doe.gov
erich.hansen@srnl.doe.gov
connie.herman@srnl.doe.gov
Joseph.Manna@srnl.doe.gov
john.mayer@srnl.doe.gov
daniel.mccabe@srnl.doe.gov
Gregg.Morgan@srnl.doe.gov
frank.pennebaker@srnl.doe.gov
Amy.Ramsey@srnl.doe.gov
William.Ramsey@SRNL.DOE.gov
michael.stone@srnl.doe.gov
Boyd.Wiedenman@srnl.doe.gov
bill.wilmarth@srnl.doe.gov
chris.martino@srnl.doe.gov
john.pareizs@srnl.doe.gov
Wesley.Woodham@srnl.doe.gov
charles.crawford@srnl.doe.gov
tommy.edwards@srnl.doe.gov
jeffrey.crenshaw@srs.gov
james.folk@srs.gov
tony.polk@srs.gov
patricia.suggs@srs.gov
Records Administration (EDWS)
thomas.colleran@srs.gov
Richard.Edwards@srs.gov
eric.freed@srs.gov
bill.holtzscheiter@srs.gov
john.iaukea@srs.gov
Spencer.Isom@srs.gov
Vijay.Jain@srs.gov
Victoria.Kmiec@srs.gov
Jeremiah.Ledbetter@srs.gov
MARIA.RIOS-ARMSTRONG@SRS.GOV
Kevin.Brotherton@srs.gov
terri.fellinger@srs.gov
jeffrey.gillam@srs.gov
barbara.hamm@srs.gov
jeff.ray@srs.gov
paul.ryan@srs.gov
Azadeh.Samadi-Dezfouli@srs.gov
hasmukh.shah@srs.gov
aaron.staub@srs.gov
celia.aponte@srs.gov
timothy.baughman@srs.gov
earl.brass@srs.gov
Azikiwe.hooker@srs.gov
Thomas.Huff@srs.gov
Ryan.McNew@srs.gov
phillip.norris@srs.gov
Christine.Ridgeway@srs.gov
arthur.wiggins@srs.gov